Climate Dynamics (2003) 21: 177–195
DOI 10.1007/s00382-003-0324-6

A. K. Pardaens · H. T. Banks · J. M. Gregory
P. R. Rowntree

Freshwater transports in HadCM3

Received: 30 August 2001 / Accepted: 14 February 2003 / Published online: 24 May 2003

Abstract The hydrological cycle can influence climate through a great variety of processes. A good representation of the hydrological cycle in climate models is therefore crucial. Attempts to analyse the global hydrological cycle are hampered by a deficiency of suitable observations, particularly over the oceans. Fully coupled general circulation models are potentially powerful tools in interpreting the limited observational data in the context of large-scale freshwater exchanges. We have looked at large-scale aspects of the global freshwater budget in a simulation, of over 1000 years, by the Hadley Centre coupled climate model (HadCM3). Many aspects of the global hydrological cycle are well represented, but the model hydrological cycle appears to be too strong, with overly large precipitation and evaporation components in comparison with the observational datasets we have used. We show that the ocean basin-scale meridional transports of freshwater come into near balance with the surface freshwater fluxes on a time scale of about 400 years, with the major change being a relative increase of freshwater transport from the Southern Ocean into the Atlantic Ocean. Comparison with observations, supported by sensitivity tests, suggests that the major cause of a drift to more saline condition in the model Atlantic is an overestimate of evaporation, although other freshwater budget components may also play a role. The increase in ocean freshwater transport into the Atlantic during the simulation, primarily coming from the overturning circulation component, which changes from divergent to convergent, acts to balance this freshwater budget deficit. The stability of the thermohaline circulation in HadCM3 may be affected by these freshwater transport changes and this question is examined in the context of an existing conceptual model.

A. K. Pardaens (✉) · H. T. Banks · J. M. Gregory
P. R. Rowntree
Met Office, Hadley Centre for Climate Prediction and Research, London Road, Bracknell, Berkshire, RG12 2SY, UK
E-mail: Anne.Pardaens@metoffice.com

1 Introduction

The hydrological cycle links four components of the Earth system: atmosphere, ocean, sea-ice and land, and can therefore influence climate through a great variety of processes (e.g. Chahine 1992; Rahmstorf 1996; Zaucker et al. 1994; Cox et al. 2000). These influences of the hydrological cycle on climate, the importance of water to life on Earth, and the potentially serious consequences for societies and ecosystems of changes to the hydrological cycle, mean that the understanding of the hydrological cycle and its accurate representation in climate models are crucial. The hydrological cycle strongly affects the radiative balance at the Earth's surface in a number of ways. In a greenhouse warming scenario the capacity of the atmosphere to store water vapour, itself an effective greenhouse gas, increases. Additionally, changes in sea-ice or snow cover impact on the radiative balance through changes in surface albedo. Feedbacks on surface temperature associated with cloud processes, which have a potentially large climatic impact, are the subject of much debate (e.g. Chahine 1992).

In the ocean, sea water consists of freshwater and salt. Net ocean volume transport, and salinity differences between northward and southward travelling sea water, both in the horizontal and with depth, constitute effective freshwater transports. Local differences in ocean salinity arising from ocean advection or from surface fluxes of freshwater contribute to density differences, which then drive the ocean thermohaline circulation. For the ocean, some model studies indicate that relatively small changes from 'present-day' surface freshwater flux into the Atlantic may be able to dramatically change the thermohaline circulation (THC) on decadal time scales (e.g. Rahmstorf 1995). A more

gradual extinction of a model THC, on century time scales, under a quadrupling of CO_2 was also found to be primarily due to increased freshwater input at high latitudes (Manabe and Stouffer 1994). Climate may change dramatically in response to collapse of the thermohaline circulation (Vellinga and Wood 2002). Greenhouse warming model simulations generally show some weakening of the THC, but the degree of weakening varies between models. It has been suggested that the behaviour of the model hydrological cycles may be responsible for these different model responses (Rahmstorf 2000; Latif et al. 2000). Investigation of the response of the THC in the HadCM3 model to greenhouse gas forcing (Thorpe et al. 2001) and to an induced collapse (Vellinga et al. 2002) show that the hydrological cycle is critical to its behaviour.

Attempts to analyse aspects of the observed hydrological cycle (e.g. Trenberth and Guillemot 1998; Wijffels et al. 1992; Wijffels 2001) and to summarize them in the context of a global system (e.g. Chen et al. 1994), have been made. Such studies, however, are hampered by the margins of error in, and availability of, observations relevant to the global hydrological cycle. Fully coupled general circulation models are potentially powerful tools for the understanding of the global hydrological cycle, as all components of the cycle can be diagnosed and are self consistent. Model freshwater cycle analysis can be used to aid interpretation of available observations in the context of global freshwater exchanges and transports. The recent advent of coupled models which do not need correction of surface heat and freshwater fluxes in order to maintain a stable climate allows the role of components of the hydrological cycle to be more usefully analysed. Here we will describe large-scale aspects of the freshwater budget in the Hadley Centre global coupled atmosphere–ocean climate model, HadCM3. Sections 2 and 3 describe aspects of the model formulation, Sect. 4 describes the climatologies used to evaluate the model. Sections 5 and 6 describe the global and regional freshwater budgets. In Sects. 7 and 8 we consider the salinity drift and freshwater budget of the Atlantic Ocean and its implications for the thermohaline circulation.

2 The HadCM3 model and its control experiment

HadCM3 is the Hadley Centre global coupled atmosphere–ocean climate model. We have analysed the control simulation (Gordon et al. 2000), of over 1000 years, which has atmospheric greenhouse gas composition appropriate to 1860. The atmosphere model (HadAM3) and the AMIP I (first Atmospheric Model Intercomparison Project) atmosphere-only model simulation referred to here are discussed by Pope et al. (2000). The atmosphere model has a resolution of 3.75° longitude by 2.5° latitude with 19 vertical levels. The ocean model is based on the model of Cox (1984) and has a resolution of 1.25° by 1.25° with 20 vertical levels. The ocean component of the coupled model was initialised with potential temperatures and salinities from Levitus and Boyer (1994) and Levitus et al. (1994) datasets and allowed to evolve from rest. The sea-ice model is on the same grid as the ocean model. The sea-ice thermodynamics is based on the zero-layer model of Semtner (1976) and simple parametrizations of ice drift and leads are included. Further details of the ocean, sea-ice and atmosphere models, including details of the model schemes relevant to the freshwater budget, can be found in Gordon et al. (2000) and Pope et al. (2000).

The horizontal resolution of HadCM3 is insufficient to simulate ocean transport through narrow straits. Wijffels et al. (1992) noted that the magnitude of the volume transport through Bering Strait is small (0.8 Sv, where 1 Sv = 10^6 m^3 s^{-1}), but that this low salinity water constitutes a significant freshwater transport. In the ocean model version used for HadCM3, there is no volume transport through the Bering Strait or net meridional volume transport around Eurasia and the Americas, constraining the means by which meridional freshwater transport can occur. In addition, the coarse resolution of the model means that the ocean passages through the Canadian Archipelago and through the narrow straits connecting the ocean basins to some of the smaller seas, such as Hudson Bay, the Baltic Sea, the Red Sea and the Black Sea, are closed. The Gibraltar Strait connecting the Atlantic to the Mediterranean is also closed, but a diffusive parametrization allows some sea water exchange across it. In order to prevent the salinities from reaching very unrealistic values in seas, such as Hudson Bay, which are cut off from the larger ocean basins in the model, the salinity is restricted to lie between 0 and 45 psu. This restriction represents a non-conservation in the global freshwater budget (discussed in Sect. 5).

The HadCM3 control experiment has run without flux adjustment for over 1000 years, with a sea surface temperature error pattern which is established quickly (mostly within the first decade) and subsequently undergoes little drift (Gordon et al. 2000). The maximum overturning stream function value of the North Atlantic Deep Water overturning cell remains fairly similar throughout the run (a mean value of 21.6 Sv over years 101–340 (Wood et al. 1999), decreasing a little later in the run) although particulars of the overturning cell shape and that of the Antarctic bottom cell change in some respects (Gordon et al. 2000). The long-term drifts in salinity discussed later have not, therefore, significantly affected the cell strength. Wood et al. (1999) found that quantities describing the THC in the control model compared fairly well with observations of the present-day circulation. We have analysed global freshwater transports for a number of model time periods (years 1–10, 81–120, 361–400, 721–760, 1081–1120). The earlier three time periods match those discussed by Gordon et al. (2000) and are at appropriate points of the model run to describe the coming into balance of the large-scale freshwater budget components both globally and in the Atlantic ocean.

3 Formulation of atmosphere and ocean freshwater transports

Freshwater can be stored in the climate system in the atmosphere, on land and in the ocean. Local storage in the atmosphere amounts to only tens of millimetres liquid equivalent, and is determined by the climate state, so changes in it are negligible on decadal time scales compared with the fluxes of precipitation and evaporation (typically of order 1 m yr^{-1}). We can therefore assume that local atmospheric water content is in a steady state in which the area-integrated evaporation (E) minus precipitation (P) (both in kg m^{-2} s^{-1}) over any given surface area (A) must equal the export of atmospheric water vapour from that area:

$$\int_A (E-P)\mathrm{d}A = \oint_{\partial A} \mathbf{Q}\cdot\mathbf{n}\,\mathrm{d}s \qquad (1)$$

where $\mathbf{n}$ is the outward unit normal along section ds of the area boundary ∂A. The atmospheric water vapour flux $\mathbf{Q}$ is calculated as

$$\mathbf{Q} = \frac{1}{g}\int q\mathbf{v}_a \,\mathrm{d}p \tag{2}$$

where q, $\mathbf{v}_a$ and p are the specific humidity, horizontal atmospheric velocity and atmospheric pressure respectively, and the integral is from the surface to the top-of-the-atmosphere.

On land, P exceeds E, but the capacity for storage of water is again small enough that changes in it can be generally neglected in decadal averages, so $P - E$ equals the local runoff, which is transported by rivers to the coast and discharged into the ocean. To close the mass balance for a land-based ice-sheet in a steady state, one must also include the solid runoff produced in the form of ice-shelves and icebergs, whose freshwater is added to the ocean as they melt. In HadCM3 this is achieved by imposing a near balance, on multicentury time scales, between the water equivalent of ice accumulating on land and a freshwater flux applied to the ocean in iceberg regions (see Gordon et al. 2000).

The net surface freshwater flux added to the ocean is $F_s = P - E + R - I$, where R is runoff (including ice from ice-sheets) and I is the rate of sea-ice formation. Sea water that freezes into sea-ice (which has a much lower salt content than sea water) is later returned to the ocean when the ice melts, but since sea-ice is in motion, it represents a freshwater transport. If the area considered includes both formation and melting, and if the sea-ice volume is in a climatological steady state, the average of I will be zero. HadCM3 experiments generally suggest that sea-ice reaches a steady state, after a climate perturbation, within a decade or two (Gregory et al. 2002). In any case, the freshwater stored in sea-ice is only of order of 1 m, so reasonable changes in sea-ice thickness occurring over decades give freshwater fluxes that are small compared with P.

Unlike the stores of freshwater in the atmosphere and on the surface, the local freshwater content of the ocean may change substantially over long time scales, during which its rate of change can be comparable with F_s. This is because salinity has no direct climate influence and is therefore not subject to rapid feedbacks. In HadCM3, however, we cannot directly keep track of the ocean freshwater content, because model sea-level is fixed as a consequence of the rigid-lid approximation used by the model of Cox (1984). Hence the model ocean volume is also fixed, and we cannot impose conservation of freshwater or salt. We can simulate only the dilution of salinity caused by addition of freshwater, not the concomitant change in volume.

The salinity of the top model layer, which has thickness h, is changed at a rate $-F_s S_*/h\rho_*$ (psu s^{-1}), as would result from adding freshwater to a depth h of water of salinity S_* and density ρ_*, assuming salt to be conserved. We express this as a surface salinity flux of $-F_s S_*/\rho_*$ (psu m s^{-1}). In the ocean interior, the real-world conditions of conservation of freshwater and salt are replaced in the model by conservation of volume and salinity, the latter satisfying

$$\int_A -F_s \frac{S_*}{\rho_*}\,\mathrm{d}A = \iint_A \frac{\partial S}{\partial t}\,\mathrm{d}A\,\mathrm{d}z + \oint_{\partial A} S\mathbf{v}_o \cdot \mathbf{n}\,\mathrm{d}s \tag{3}$$

where S and $\mathbf{v}_o$ are salinity and ocean velocity and the z-integral is over the complete depth of the model ocean. In the model, diffusion as well as the resolved advection contributes to the ocean salinity transport, but the latter is dominant. Implications of the formulation are briefly discussed in Appendix 1.

In the real ocean, a steady state implies zero divergence of salt, and a mass divergence which balances the surface freshwater mass flux, the latter condition being equivalent to conservation of volume if we assume constant density. In an unsteady state, while salinities are changing, there may be both a salt divergence and a volume divergence. Adjustment to a new state will involve both change in salinity and change in sea-level (as a consequence of volume divergence). The constraint of constant volume in the HadCM3 ocean means that it is not strictly possible to say whether a model salinity divergence in an unsteady state represents a salt divergence, a freshwater divergence, or a combination of the two.

In the real ocean, in a steady state, conservation of mass in an area A bounded by cross sections X_i gives

$$\int_A F_s\,\mathrm{d}A = \oint_{\partial A} \rho\mathbf{v}_o \cdot \mathbf{n}\,\mathrm{d}s = \sum_i \int_{X_i} \rho\mathbf{v}_o \cdot \mathbf{n}_i\,\mathrm{d}X_i \tag{4}$$

and conservation of salt

$$0 = \sum_i \int_{X_i} \rho S\mathbf{v}_o \cdot \mathbf{n}_i\,\mathrm{d}X_i \ . \tag{5}$$

Hence subtracting Eqs. 4 from 5, $\int_A F_s\,\mathrm{d}A = \sum_i F_{Xi}$, where $F_{Xi} \equiv \int_{X_i} \rho(1-S)\mathbf{v}_o \cdot \mathbf{n}_i\,\mathrm{d}X_i$ is the freshwater transport through X_i. If two sections bound the volume (e.g. two zonal sections across an ocean basin), $F_{X2} = -F_{X1} + \int_A F_s\,\mathrm{d}A$, i.e. the outflow F_{X2} is the sum of the inflow $-F_{X1}$ and the surface water input. This formula can be applied to surface freshwater flux observations to compute the freshwater transport through one section (say F_{X2}) given the value (F_{X1}) for another section, and this is the approach of Wijffels et al. (1992). Applying the formula by analogy to the model, we call F_{X2} the 'implied' ocean freshwater transport through X_2, indicating that this transport is what is required to balance the surface water flux.

From Eq. 3, in a steady state, transports of salinity S_{Xi}, where $S_{Xi} \equiv \int_{X_i} Sv_o \cdot n_i\,\mathrm{d}X_i$, through the two model sections satisfy $-(\rho_*/S_*)(S_{X1} + S_{X2}) = \int_A F_s\,\mathrm{d}A = F_{X1} + F_{X2}$and hence $F_{X2} = -F_{X1} - (\rho_*/S_*)(S_{X1} + S_{X2})$. We call F_{X2} calculated this way the ocean or 'direct' ocean freshwater transport, because it is diagnosed from ocean velocities. Disagreement between implied and direct transports indicates a drift in salinity i.e. an unsteady state. Note that we do not equate $-(\rho_*/S_*)S_{Xi}$ to F_{Xi}; it is only the *divergences* in freshwater and salinity transport that are equated i.e. $-(\rho_*/S_*)\sum_i S_{Xi} = \sum_i F_{Xi}$.

4 Climatologies used for model evaluation

The climatologies of the directly observed components of the freshwater budget do not have global coverage. We have compared the model with observations in the regions where these coincide. For precipitation, we have used an annual mean climatology from the CMAP/O 1979–1998 dataset (Xie and Arkin 1997) for model evaluation. The CMAP/O product merges satellite and gauge based analyses to produce a precipitation climatology. Precipitation is not well monitored in the mid- to high-latitude regions and the differences between the CMAP/O climatology and an alternative CMAP product climatology, which includes data from the NCEP-NCAR reanalyses, are referred to. We have calculated an annual mean evaporation field over the ocean using the latent heat field from the Southampton Oceanography Centre (SOC) ship-based measurement climatology (Josey et al. 1999) which was created using correction for known measurement biases to individual observations. We concentrate on the Atlantic (to 30°S) for much of our analysis, and this region is relatively well covered by ship data (see Josey et al. 1999). For runoff we have mainly used the estimates given by Baumgartner and Reichel (1975) which are provided for each ocean basin in 5° latitude bands.

The $P - E$ climatology over the oceans, formed from the CMAP/O precipitation and SOC evaporation, is not constrained to be in global balance with the observed estimates of runoff into the oceans from Baumgartner and Reichel (1975). A rough estimate of this imbalance, using the difference between model oceanic $P - E$ (which is close to global balance with model runoff) and observed $P - E$ over their common area, gives an imbalance of approximately 1.37 Sv (equivalent to about 0.37 mm day^{-1}, which is about 14% of the global CMAP/O precipitation). The origins of the imbalance in the climatological surface flux freshwater budget data are not obvious. In the SOC heat flux climatology, Josey et al. (1999) find a global gain of $+30$ W m^{-2} by the ocean. There is some suggestion of a similar magnitude excess heat flux from these surface climatologies relative to ocean section heat flux divergence estimates in the tropical and subtropical Atlantic (see Fig. 8 of Josey et al. 1999). If such a difference were entirely due to errors in the latent heat component, an increase in observed evaporation of

approximately 1 mm day^{-1} would be needed. Josey et al. (1999) conclude, however, that various regionally dependent processes are likely to contribute to the imbalance in their climatological global heat budget, and that simple global adjustments of the bulk formulae, as provided by da Silva et al. (1994) to give a globally balanced observed heat and freshwater budget, can lead to greater biases when comparing the latent heat flux with estimates derived from buoy measurements. For comparison with estimates from these surface freshwater flux climatologies, we have also referred to the ship-based precipitation and evaporation climatologies of da Silva et al. (1994), and the Trenberth and Guillemot (1998) $P - E$ climatology (T42 version now available and used), which is derived from the atmospheric moisture transports in the NCEP-NCAR reanalyses and so is not directly dependent on surface flux parametrizations. We have also used other estimates of runoff, and some of $P - E$, into the Mediterranean (da Silva et al. 1994), Hudson and James Bay (Prinsenberg 1980) and into the Baltic (Eilola and Stigebrandt 1998) to infer the loss of freshwater due to unrealistically closed model straits, and to adjust Baumgartner and Reichel (1975) estimates of runoff to an Atlantic basin area without these connecting seas.

For our investigation of the Atlantic freshwater budget, we have made use of a number of estimates of freshwater transport derived from ocean sections: Bering Strait (Coachman and Aagaard 1988, freshwater transport as given by Wijffels et al. 1992); Atlantic 55°N section (Bacon 1997); Atlantic 24°N section (Hall and Bryden 1982, using calculations by Saunders and King 1995); Atlantic 11°N section (Friedrichs and Hall 1993, used their annual mean freshwater transport estimate); seven Atlantic sections between 40°S and 11°S (Holfort and Siedler 2001); estimates from Koltermann et al. (1999) for sections in the Northern Hemisphere Atlantic (we have not included the estimates from 1950s data as the authors suggest that differences between these and the estimates from 1980s and 1990s data are probably due to poor spatial resolution of the 1950s data), and an estimate for the Strait of Gibraltar (Bryden et al. 1994). Some of the estimates derived from ocean sections are in fact from inverse models, in which hydrographic sections, surface flux estimates and a physical model are adjusted to be consistent and used to estimate transports of ocean constituents.

There is considerable uncertainty in the magnitude of the freshwater budget components for the ocean basins. The errors relevant to available observations are discussed in Wijffels (2001) and several illustrations of the degree to which the available climatologies differ are presented there. Freshwater transport convergences between ocean sections estimated from surface fluxes have an error that is dependent on surface area between the sections. Convergence estimates derived from ocean section measurements also have errors and inaccuracies associated with them, but do not have this area dependent problem. Wijffels (2001) finds that, when integrated over the Atlantic between 40°S and the Bering Strait, the implied (from surface flux climatologies) ocean freshwater transport convergence ranges between approximately 1 and –0.1 Sv while the direct estimates indicate very little freshwater convergence between these latitudes. An estimate derived from ocean sections and an inverse model that has appeared more recently, however, suggests a convergence of about 0.26 Sv (Holfort and Siedler 2001). Wijffels (2001) estimates that the uncertainty in the freshwater flux into an ocean basin derived from direct ocean section freshwater transport estimates might be as large as +/– 0.17 Sv using sections outside of the tropics, and reach +/–0.3 Sv using sections in the tropics.

5 The global freshwater budget

The HadCM3 freshwater fluxes of precipitation and evaporation over the global land and ocean/sea-ice surfaces, and the runoff (including iceberg melt) to the ocean, are shown in Fig. 1 for years 361–400 (they remain very similar for the other time-mean periods analysed). The global precipitation is equivalent to approximately 2.90 mm day^{-1}. Table 1 shows the freshwater budget for just the interconnected model ocean basins (including the Mediterranean which is connected by a diffusive transport but excluding, for example, Hudson Bay which is enclosed in the model). Note that the contribution shown from the sea-ice model to these totals is mostly due to the intercepted snowfall (precipitation falls as snow onto the sea-ice and subsequently melts into the ocean), as the change in sea-ice volume through the run is small. While the total freshwater flux into the ocean and sea-ice surface is near zero (0.0006 Sv for years 361–400), there is a larger imbalance for the interconnected ocean regions (see Table 1), due mainly to the closure of some straits which are not resolved by the model grid. The implications of this for the Atlantic are discussed in Sect. 7. The change in global ocean volume-averaged salinity is less than 0.01 psu over the first 1000 years of the simulation. Further details of the conservation of water in HadCM3 are discussed in Gordon et al. (2000).

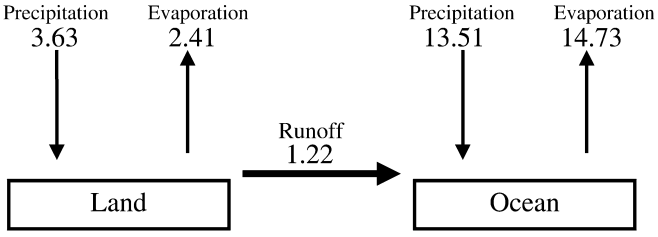

Fig. 1 HadCM3 freshwater fluxes (in Sv) of precipitation and evaporation over the global land and ocean/sea-ice surfaces and of runoff (river and iceberg contributions) from land to ocean for model years 361–400

Table 1 HadCM3 control simulation surface freshwater into the interconnected ocean basins (Sv) for years 1–10 and 361–400. The '$P - E$ directly to ocean' term does not include that which falls as snow onto the sea-ice and subsequently melts, this appears in the 'Sea-ice + intercepted snowfall' term

Years	$P - E$ directly to ocean	Runoff + iceberg	Sea-ice + intercepted snowfall	Total
1–10	–1.38	1.11	0.18	–0.10
361–400	–1.41	1.15	0.24	–0.03

Comparing model and observed surface freshwater fluxes averaged over their common global areas gives higher model precipitation and evaporation than observed (precipitation by about 0.26 mm day^{-1} relative to the CMAP/O 2.69 mm day^{-1} and evaporation by approximately 0.62 mm day^{-1} relative to SOC 3.18 mm day^{-1}). Uncertainties in the data are too large to conclude this with any confidence, but other model behaviour which suggests this has also been found. The distribution of salinity per unit volume of the global ocean tends to more extreme values as the model run progresses, suggesting either a deficiency in ocean

mixing or an overly strong model hydrological cycle. The globally averaged HadCM3 salinity error with depth relative to Levitus et al. (1994) is shown in Gordon et al. (2000) (their Fig. 3b). It shows that below 1000 m the ocean gets progressively more saline, while above this the ocean becomes too fresh. This error profile could be consistent with deficiencies in mixing or with an enhanced global hydrological cycle. If fresh and saline errors are created near the surface by too much precipitation or evaporation in different regions, the overly saline water masses will tend to sink because they are denser than the overly fresh water masses. Errors in the global potential density profile with depth (not shown) indicate that the model potential density is too low near the surface and too high at depth.

Much of the SSS error pattern (shown in Fig. 2 for three time periods) is established within the first decade of the model simulation, but the fresh errors generally increase in magnitude and area over the first three to four hundred years while the surface saline errors tend to remain similar or be eroded. After this period the drifts are much reduced. The most notable exceptions to this surface freshening trend are in the Mediterranean (discussed further in Sect. 7), where an increase in surface salinity during the simulation is evident, and in some seas which are unrealistically cut off from the main ocean basins (e.g. the Red Sea).

Figure 3 shows the global northward direct ocean and implied freshwater transports in the initial model decade and for the time mean of years 361–400. Differences between these are an indicator of the degree of balance in the model freshwater budget (see Sect. 3). The direct meridional transport of freshwater by rivers, sea-ice and by the representation of the iceberg water flux are also shown for years 361–400. The transports implied by the surface fluxes (which remain similar through the model run) undergo relatively little change compared to the direct ocean transports. The implied global ocean meridional freshwater transports are evidently not in balance with the direct ocean transports at the beginning of the run, but by years 361–400 a relative increase in northward ocean transport of freshwater in the Southern Hemisphere and low latitudes of the Northern Hemisphere leads to a balance at most latitudes. In this global mean sense, the meridional transports approach balance after about 150 years, but on the scale of the individual ocean basins, the freshwater budgets balance on a time scale closer to 400 years (see Sect. 6.4). Such a balance indicates that the drifts of basin volume-averaged salinity are small (see Sect. 3), but it does not exclude more local compensating drifts within the basins.

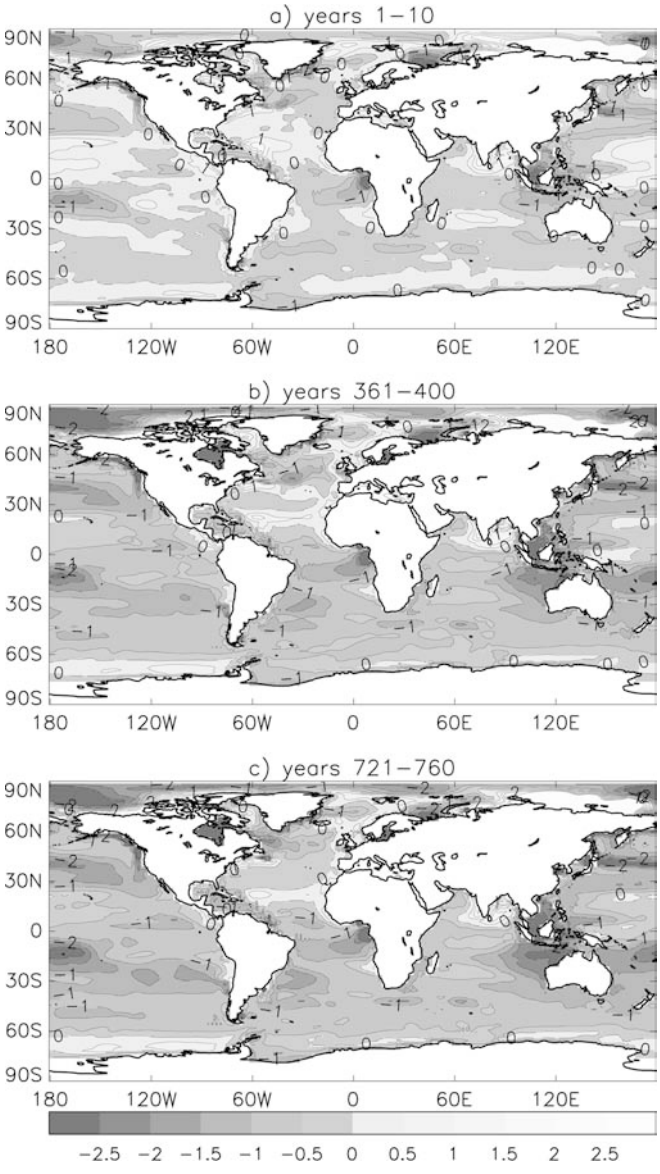

Fig. 2 HadCM3 sea surface salinity error (contours every 0.5 psu) from Levitus et al. (1994) climatology for **a** years 1–10, **b** years 361–400, **c** years 721–760

6 Regional freshwater fluxes

In the following sections we describe the differences from observations of the water fluxes from precipitation, evaporation, river runoff and sea-ice in HadCM3. Regional variations in sea surface salinity are known to be strongly related to regional variations in surface freshwater fluxes (e.g. Chen et al. 1994), and so errors in the surface freshwater fluxes are also likely to be reflected in surface salinity errors (shown in Fig. 2). As noted in Sect. 5, however, the near surface salinity errors may more readily reflect positive (into the ocean) surface flux errors than negative (out of the ocean) surface flux errors (which, other things being equal, will tend to sink). We show the freshwater transported by the atmosphere (as water vapour), by rivers and by the ocean into large-scale ocean basin analysis areas (with regions referred to as labelled in Fig. 10) to illustrate the model freshwater cycle.

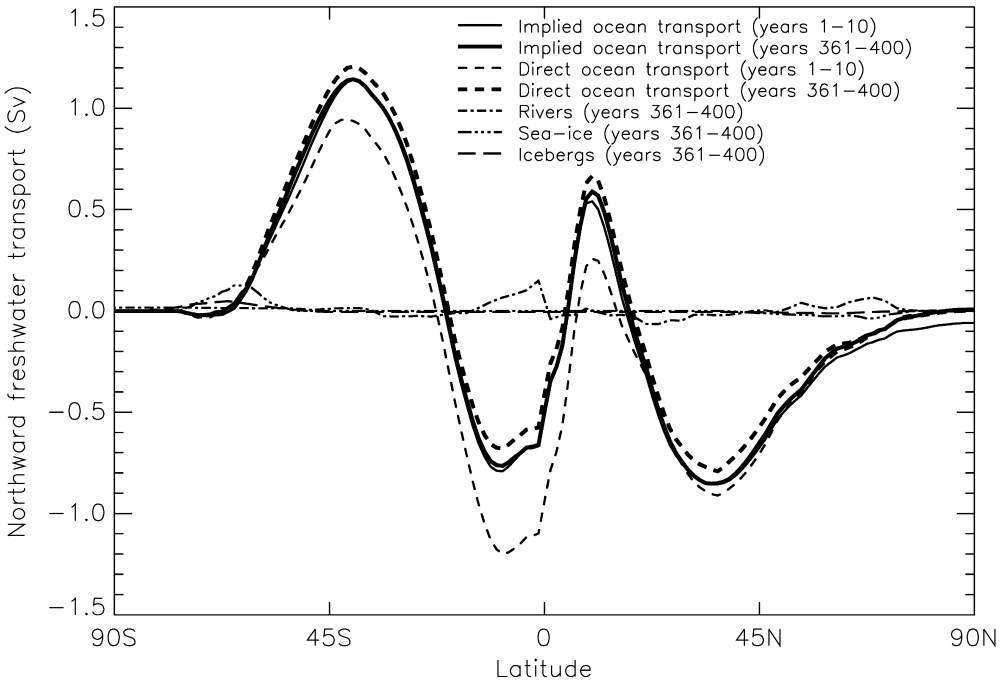

Fig. 3 Global HadCM3 direct and implied oceanic meridional freshwater transports, and meridional transports of freshwater by rivers, sea-ice and by the iceberg freshwater flux representation

6.1 Precipitation, evaporation and atmospheric water vapour transport

The coupled model $P - E$ field (Fig. 4) is similar on decadal-type time scales throughout the model run, consistent with the lack of significant drifts in the sea surface temperature (SST) and sea-ice extents after the initial decade (Gordon et al. 2000). The spatial pattern of model $P - E$ error relative to observations (Fig. 4a) largely reflects precipitation errors (Fig. 5), but with negative surface flux errors generally emphasised due to an overestimate of evaporation (Fig. 6) in the tropical–subtropical belt. Too much tropical and subtropical evaporation is evident relative to the SOC climatology (Fig. 6) in both coupled and atmosphere-only (not shown) models, but the evaporative errors are enhanced over the coupled model warm SST error regions (SST errors are shown in Fig. 6 of Gordon et al. 2000) and often reduced or even change sign in the coldest SST error regions.

At mid to high latitudes the coupled model precipitation tends to be overestimated compared to CMAP/O (Fig. 5c) and this is also true of the AMIP version of this model. This HadCM3 precipitation error, which dominates the $P - E$ error (Fig. 4a) at the higher latitudes, would lead to too large a freshwater input to the ocean in these regions. In the Southern Ocean, between 50 and 60°S (the southernmost limit of the CMAP/O climatology), the annual mean precipitation in HadCM3 is generally too high by > 1 mm day^{-1}, and by > 1.5 mm day^{-1} in some locations but, as noted in Sect. 4, there is little observed data in this region. The CMAP precipitation climatology, which includes reanalysis data, has higher precipitation at the northern and southern high latitudes than CMAP/O, and a comparison of HadCM3 against CMAP would reduce, but not eliminate, the magnitude of excessive model precipitation in the Southern Ocean. Integrating the Trenberth and Guillemot (1998) $P - E$ over the Southern Ocean region south of 30°S gives 0.68 Sv which is only about 0.05 Sv less than that given by the coupled model, but this estimate may be dominated by the reanalysis model. Ocean sections can also give us information about the freshwater budget in the Southern Ocean and are discussed in Sect. 6.4.

In the tropical–subtropical regions, the coupled model $P - E$ and precipitation error patterns (Figs. 4a, 5c) are similar in the tropical–subtropical regions to the differences between the coupled and atmosphere-only model $P - E$ (Fig. 4c) or precipitation, consistent with some control on precipitation errors, via convection, by coupled model SST errors. The coupled model precipitation error, for example, is positive over the maritime continent, where the coupled model SSTs are too warm. In general, however, there is an overestimate of evaporation at lower latitudes and an overestimate of precipitation at higher latitudes, relative to the CMAP/O and SOC climatologies, in both coupled and atmosphere-only models, which are consistent with an overly strong hydrological cycle. The HadCM3 $P - E$ errors are, in many respects, reflected in the coupled model SSS error field with respect to Levitus et al. (1994) (Fig. 2), particularly at the lower latitudes and in the first decade, before a fairly general surface freshening takes place.

Chen et al. (1994) analysed the interbasin transport of water vapour using operational analysis data (see their Fig. 3b). In a similar way, Fig. 7 shows $\tilde{Q}_D$,the divergent component of vertically integrated water vapour transport summed along boundary sections of the large-scale ocean basin analysis areas that we are using to illustrate the model freshwater cycle. Using the notation of Sect. 3,

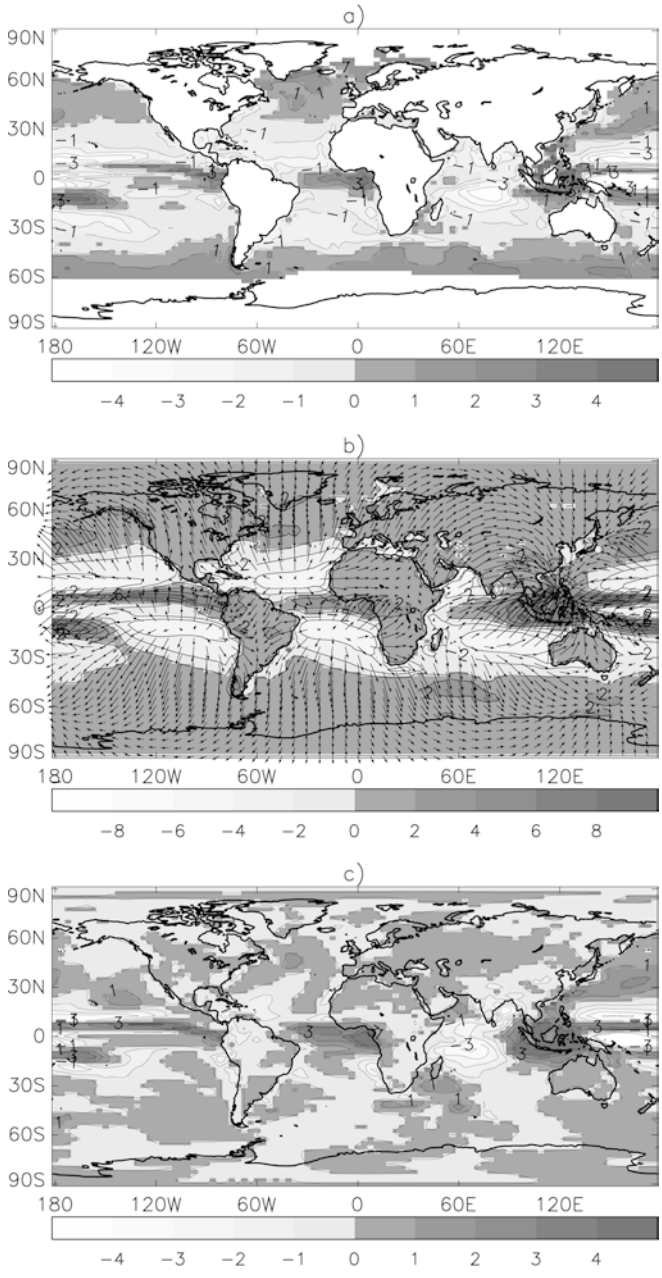

Fig. 4 **a** HadCM3 $P - E$ error from climatology (CMAP/O precipitation, SOC evaporation) for years 361–400 (contours every 1 mm day^{-1}), **b** HadCM3 $P - E$ for years 361–400 (contours every 2 mm day^{-1}), with vectors of the divergent component of vertically integrated water vapour flux ($\mathbf{Q}_D$) overlaid, **c** Difference field of HadCM3 minus HadAM3 $P - E$ (contours every 1 mm day^{-1})

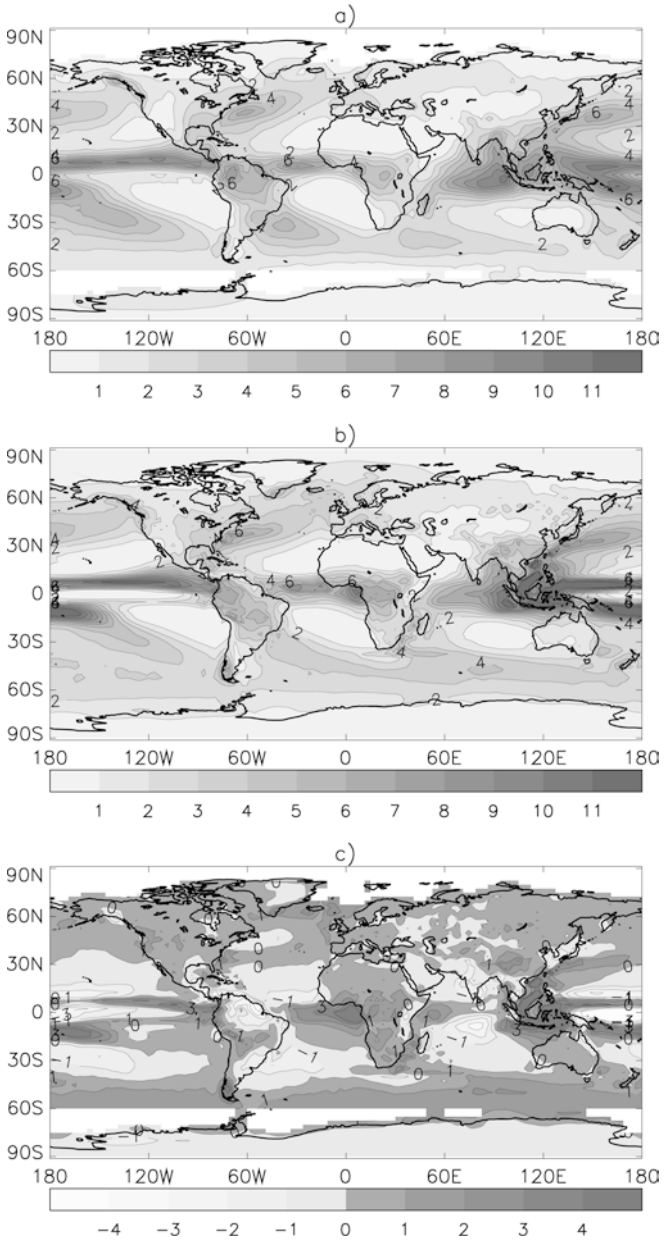

Fig. 5 Precipitation (contours every 1 mm day^{-1}) **a** CMAP/O climatology for 1979–1998, **b** HadCM3 for years 361–400, **c** difference field of HadCM3 minus CMAP/O

the divergent water vapour transport, $\mathbf{Q}_D$, is the component of $\mathbf{Q}$ that links directly to the $P - E$ budget, with $Q = Q_D + Q_R$, $\tilde{Q}_D = \left|\int Q_D \cdot n \, \mathrm{d}s\right|$, and subscripts D and R referring to the divergent and rotational components respectively. The area-integrated $P - E$ and the sum of the boundary $\tilde{Q}_D$ entering the region (atmospheric model diffusion and some calculation inaccuracies lead to differences between these quantities) are also shown in Fig. 7. The model tropical–subtropical Atlantic is the dominant net evaporative region in this large-scale area-integrated $P - E$ analysis, with the Indian Ocean also a significant net evaporative region. The combined Southern Ocean regions receive a significant input of freshwater from $P - E$, due to a convergence of water vapour which has been transported from the more evaporative tropical–subtropical regions. Much of the freshwater evaporated from the Atlantic and Indian Oceans, however, returns to the ocean as river runoff (the large $\tilde{Q}_D$ exported westward over South America from the low-latitude Atlantic does not enter the Pacific basin). In the Atlantic (30°S to 66°N), model $\tilde{Q}_D$ is outbound from the basin along all of the large-scale boundary sections shown, similar to the results of

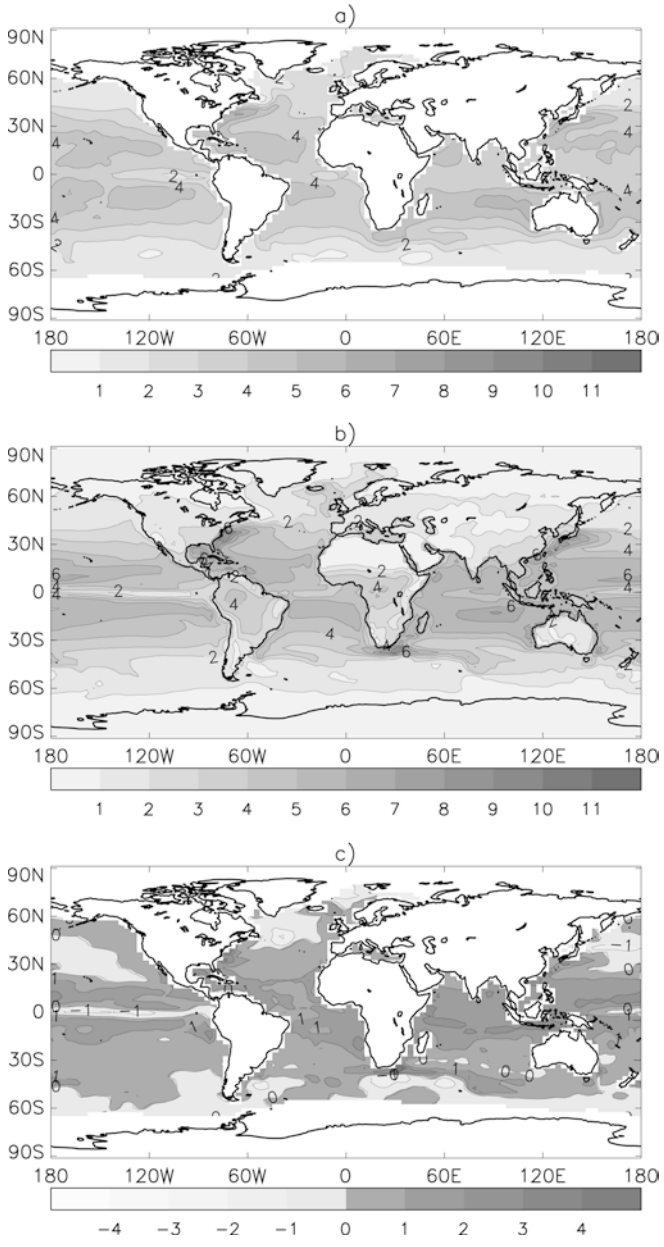

Fig. 6 Evaporation (contours every 1 mm day^{-1}) **a** SOC climatology, **b** HadCM3 for years 361–400, **c** difference field of HadCM3 minus SOC

Chen et al. (1994), with particularly large exports to the east, west and south of the tropical–subtropical region. In contrast to the Atlantic, the Pacific loses only a small $\tilde{Q}_D$ at the eastern side of the basin in the tropics-subtropics and gains a large $\tilde{Q}_D$(0.33 Sv) at the western side, transported from the Indian Ocean, also similar to the results of Chen et al. (1994).

6.2 Runoff

The runoff (including iceberg melt) into the model global ocean for years 361–400 is 1.22 Sv, which is very close to (0.04 Sv less than) the estimate for global runoff from Baumgartner and Reichel (1975). Table 2 shows large-scale area-integrated runoff for the model and estimates derived from Baumgartner and Reichel (1975). The agreement is remarkably good.

Differences in model river runoff from Baumgartner and Reichel (1975) estimates for the tropical–subtropical Atlantic are mainly due to deficiencies in the model runoff for northern South America, which is balanced in part by excessive runoff from west Africa. Figure 8 shows the runoff to the coastal boundaries of the same regions as used to look at water vapour transport in Sect. 6.1. For comparison with the 0.15 Sv and 0.22 Sv of model runoff from the east and west coasts of the tropical–subtropical Atlantic region respectively, Baumgartner and Reichel (1975) give values of 0.09 Sv (east coast) and 0.33 Sv (west coast, including runoff from the Caribbean islands).

We have made further estimates of the west coast tropical–subtropical runoff using a combination of estimates of observed runoff from river gauging stations (UNESCO 1971), and estimates of runoff in areas not covered by gauging stations derived from precipitation and evaporation estimates (from Delire et al. 1997, or calculated from using runoff and precipitation estimates in adjacent basins). These give varying estimates of the total west coast runoff which show uncertainty in the observed runoff but suggest that the coupled model underestimates the runoff. In the atmosphere-only model simulation our calculations suggest that there is also a deficiency in runoff from the Amazonian region, although the precipitation is thought to be near observed (Gedney et al. 2000).

Runoff errors estimated for the coupled model vary in sign geographically. Analysis of precipitation errors suggests that these are responsible for much of the runoff error. There is excessive precipitation and runoff over China and over much of North America and Africa. Rainfall and runoff deficiencies are evident over northern South America. Over northern Asia, however the deficiencies in runoff are commonly associated with excessive precipitation implying that the evaporation there is also excessive.

6.3 Sea-ice

Apart from scattered in-situ observations from field campaigns, there are no measurements of the surface water fluxes resulting from sea-ice processes. A comparison of model sea-ice concentration with the observed climatology (see Fig. 10 of Gordon et al. 2000) shows that the area of ice at the minimum (September in the Northern Hemisphere, February in the Southern Hemisphere) compares favourably with SSM/I data (NSIDC 1989), but that the maximum extents (March in the Northern Hemisphere, October in the Southern Hemisphere) are too great in both hemispheres. Consequently the seasonal range of ice concentration is exaggerated in

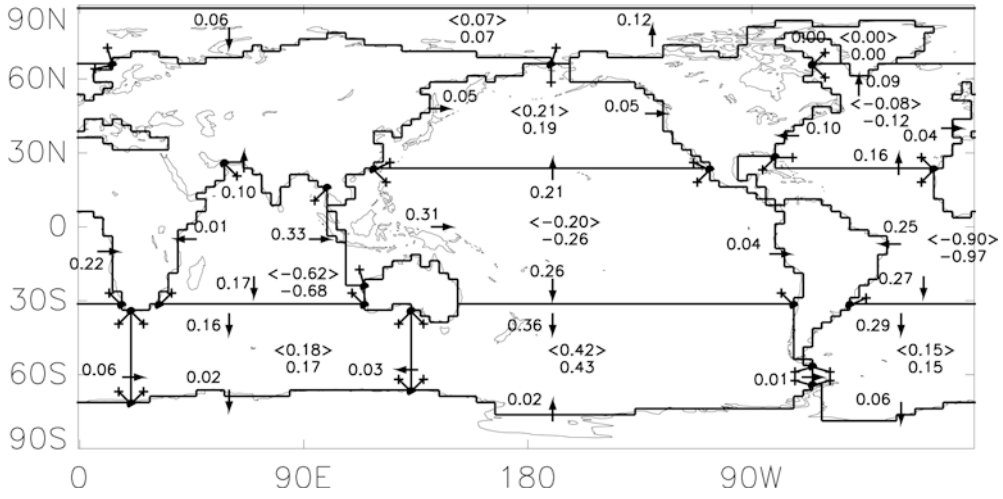

Fig. 7 HadCM3 divergent transports of water vapour ($\tilde{Q}_D$) into the large-scale ocean basins analysis areas for years 361–400 (units Sv). The analysis areas are bounded by *thicklines* (see Fig. 10 for terms used for the analysis areas). The transport shown next to an *arrow* within each analysis area has been integrated between the points marked on the area boundary which are connected to *crosses* within the relevant region. The $P - E$ and the sum of the fluxes across the bounding sections (marked by $< >$) are shown within each area (in steady state and without horizontal diffusion these quantities should be equal)

many locations, especially the Greenland, Barents, Bering and Okhotsk seas in the Northern Hemisphere, and at most longitudes in the Southern Hemisphere.

For further evaluation, we can compare the annual average water flux from ice processes in HadCM3 (see Fig. 9) with the same quantity as simulated by models which have a higher spatial resolution, more detailed ice physics, and surface forcing derived from observations; such models may consequently produce a better climatology of ice concentration and thickness. The sea-ice models of Fichefet and Morales-Maqueda (1997) and Harder et al. (1998) both use the viscous-plastic rheology of Hibler (1979) and are driven with observationally derived atmospheric forcing data. Both these models have a positive net ice growth rate over most of the Arctic basin, exceeding 0.5 m yr^{-1} over substantial regions with values of greater than 1 m yr^{-1} on the eastern side. (Note that 1 m yr^{-1} of freezing is equivalent to 2.5 mm day^{-1} of freshwater withdrawal). In contrast, HadCM3 (see Fig. 9a) has net melting over the Beaufort Sea, and net ice production does not exceed 0.5 m yr^{-1} anywhere except in regions near the coasts. Furthermore, net melting in the Greenland Sea is rather small in HadCM3 compared with the values of 2 m yr^{-1} in the other models.

These comparisons suggest that although the seasonal in-situ production and melting of sea-ice may be too large, in the annual mean too little ice is produced in the Arctic and too little melted in the Greenland Sea, which implies that the export of ice from the Arctic is deficient (see also Cattle and Cresswell 2000). In HadCM3 the export of sea-ice through the Fram Strait amounts to 0.03 Sv on average (freshwater equivalent). Using ice thickness derived from upward-looking sonar, Vinje et al. (1998) give an average of 0.090 Sv for 1990–1996, noting that there is very large interannual variability. Aagaard and Carmack (1989) suggest a figure of 0.088 Sv, with an uncertainty of perhaps 20%. The model of Harder et al. (1998) exports an average of 0.086 Sv. Miller and Russell (2000) quote an export of 0.04 Sv for their global coupled ocean–atmosphere model. Since the Fram Strait ice export is one of the largest components of the freshwater budget of both the Arctic Ocean and the Greenland Sea, we must expect some Arctic salinity errors in HadCM3 from this deficiency. Comparison of the ice thickness and velocity fields of HadCM3 with the models of Fichefet and Morales-Maqueda (1997), Steele et al. (1997) and Harder et al. (1998) suggests that the velocities, of order 0.1 m s^{-1}, are reasonable, and the ice flux is too small mainly because the ice is too thin. In the East Greenland current its thickness exceeds 1 m only in a very narrow band, whereas this should be the minimum thickness in the Fram Strait. Modelled ice export from the Arctic south of Svalbard

Table 2 Observed and modelled runoff, including iceberg melt (in Sv), for the ocean regions (as labelled in Fig. 10). The model values are from years 361–400. The observed values are taken from Baumgartner and Reichel (1975), but adapted to the model regions identified, using additional runoff data to enable this where necessary (see Sect. 4 for details)

Model/ climatology	Northern Atlantic	Tropical/ subtropiocal Atlantic	Northern Pacific	Tropical/ subtropiocal Pacific	Indian Ocean	Arctic + Baffin	Southern Ocean
HadCM3	0.095	0.370	0.148	0.153	0.115	0.104	0.151
Observed	0.098	0.412	0.140	0.206	0.128	0.106	0.125

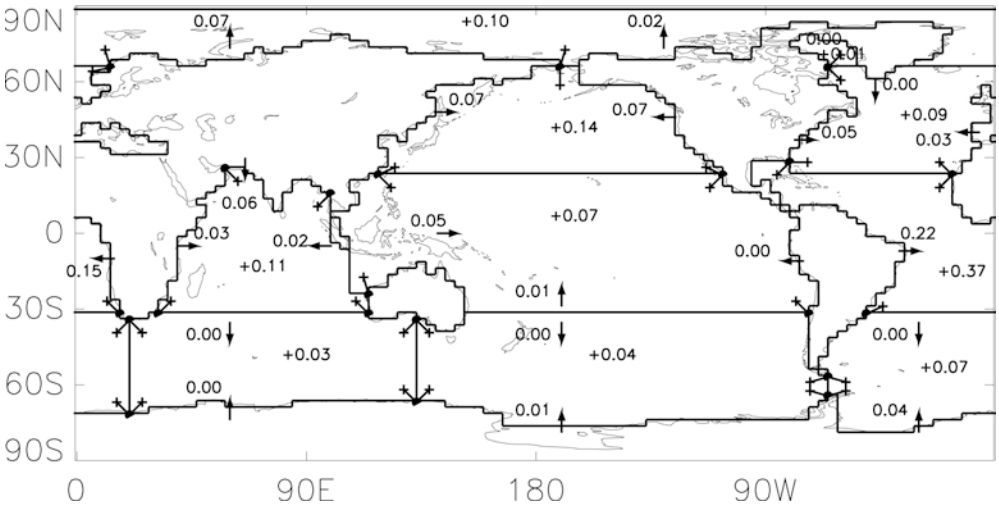

Fig. 8 HadCM3 runoff (units Sv) across the boundaries of the large-scale ocean basin analysis areas (not including runoff from islands within the areas) for years 361–400. Fluxes across boundaries which do not include any coastline have not been marked as the runoff is zero across these sections. Symbols are as for Fig. 7. The total runoff across the bounding sections added to the iceberg flux for the region (see Sect. 6.2) is shown in the *centre* of each analysis area

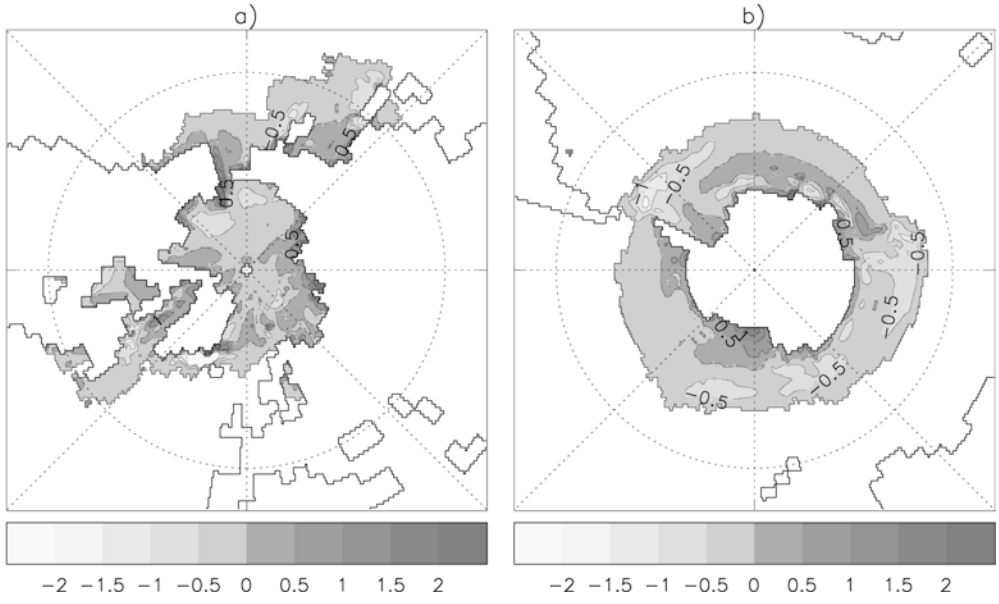

Fig. 9 Annual average water flux due to sea-ice model processes in HadCM3 for years 361–400, with contours every 0.5 m yr^{-1} equivalent of freshwater transfered out of the ocean **a** for the Arctic, **b** for the Antarctic

and through the Bering Strait is much smaller than through the Fram Strait, in accordance with observations.

In the Antarctic (Fig. 9b), HadCM3 is in good qualitative agreement with Fichefet and Morales-Maqueda (1997). Ice is produced at all latitudes round the continent, at rates of up to about 1 m yr^{-1} near the coast, and melts at lower latitudes. The region of net freezing is perhaps larger in HadCM3 than in the model of Fichefet and Morales-Maqueda (1997); the region of net melting extends to lower latitudes and shows greater values, of up to about 1 m yr^{-1}. Together these points suggest that the ice transport, and therefore effective freshwater transport, northwards from the Antarctic coast is probably too great in HadCM3.

6.4 Ocean freshwater transport

Figure 10 shows the model ocean freshwater transports (advective plus diffusive) across bounding sections of the ocean basin large-scale analysis areas for years 1–10 and 361–400 (the values for years 1–10 are from a recent scientifically near-equivalent simulation with additional diagnostics of the diffusive transport). The diffusive component is the freshwater transported by the horizontal component of isopycnal diffusion and by the effective transport given by the model's Gent and McWilliams (1990) adiabatic thickness diffusion. The ocean freshwater convergence and the salinity drift for the bounded ocean volume in terms of excess of freshwater are also shown in Fig. 10. As discussed in Sect. 3, the ocean freshwater transport convergence in steady state should be well represented by the model rigid-lid formulation. In order to show the model ocean transports of freshwater across coast-to-coast sections using the transport convergences, we have therefore introduced three variables, F_b the freshwater transport through the Bering Strait, F_p the freshwater transport across the Indonesian throughflow passages and F_a the freshwater transport through the Drake Passage. This

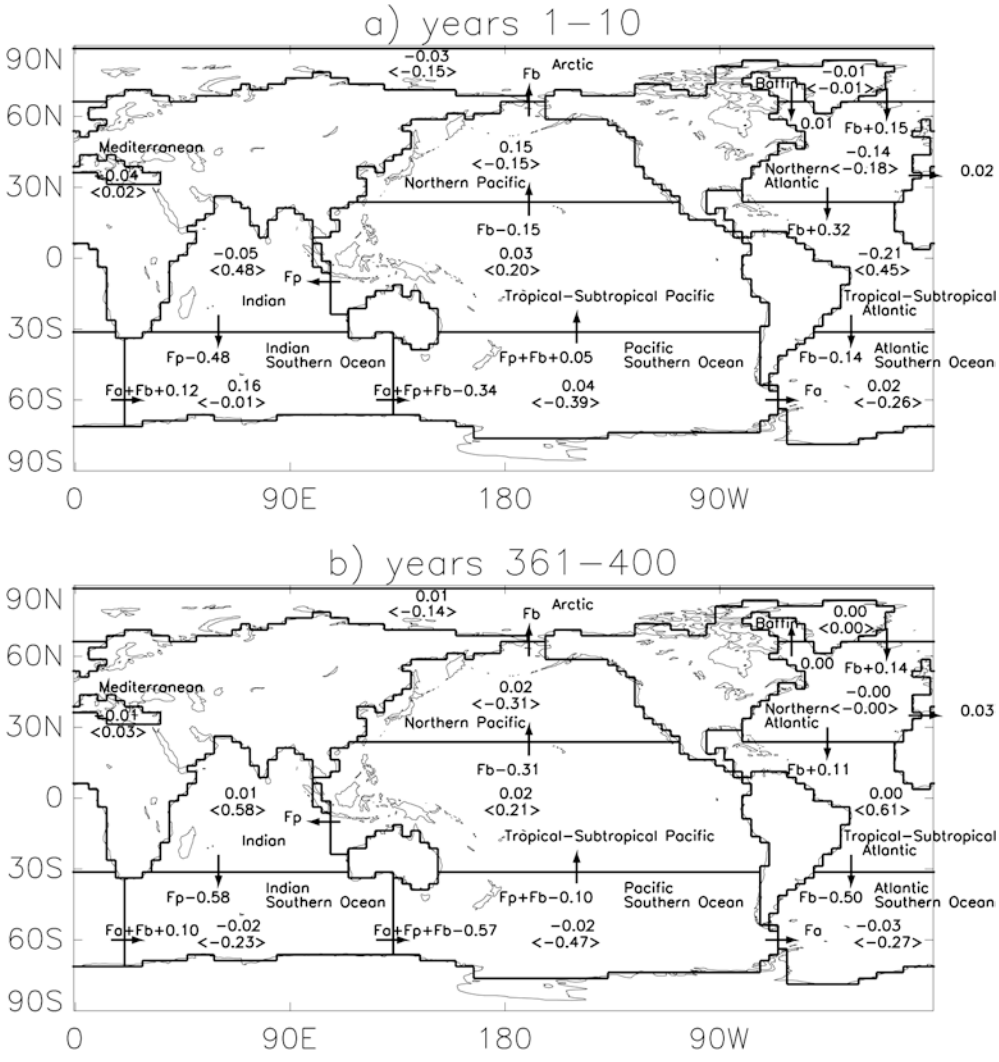

Fig. 10 HadCM3 ocean freshwater transports (units Sv) across sections bounding the large-scale ocean basin analysis areas. The terms used for the analysis areas are included on the figure. The ocean freshwater transport convergences(< >) and the excess of freshwater in the area freshwater budget (a non zero number indicates a salinity drift) are marked in the *centre* of the analysis areas **a** years 1–10, **b** years 361–400

approach is, therefore, similar to that taken by Wijffels et al. 1992 (see Sect. 3) except that they used implied rather than direct ocean freshwater convergences to construct their ocean freshwater transport scheme.

The volume-averaged salinity drifts for the ocean regions (Atlantic drifts are discussed in detail in Sect. 7) are initially dominated by salinity changes in the upper 1000–2000 m of the ocean, but after about 200–400 years, the drifts are reduced and sometimes change sign as salinity changes in the deeper ocean play a role. A comparison of Fig. 10a, b shows that in some regions notable changes to the ocean transport convergences take place in the first 400 years of the model run, which give rise to the change in global meridional ocean freshwater transport evident in Fig. 3 and reduce the basin salinity drifts (later periods analysed show relatively similar freshwater convergences in most areas to those for years 361–400). The largest basin-scale changes are an increase in the freshwater divergence from the Southern Ocean (south of 30°S) from 0.66 Sv to 0.96 Sv and an increase of freshwater convergence to the combined Arctic–Atlantic (to 30°S) region from 0.14 Sv to 0.5 Sv. The increased freshwater divergence from the Southern Ocean which brings the model direct and implied global meridional ocean freshwater transports closely into balance (see Fig. 3), is therefore predominantly acting to increase the freshwater convergence in the Atlantic ocean. The mechanisms by which the changes occur in the Atlantic and the time scales of adjustment are discussed in Sects. 7 and 8.

Comparison with observations (Sect. 6.1) suggested that the model precipitation and $P–E$ were too high in the Southern Ocean, but there are very limited surface flux observations in this region. We can, however, also compare the Southern Ocean freshwater budget with ocean section information. Sloyan and Rintoul (2001) used an inverse model, which included nine hydrographic sections, to obtain estimates of ocean freshwater export from the Southern Ocean, adjusting the surface flux estimates to be consistent with the hydrography. This method suggested an ocean freshwater export of 0.54 Sv from the Southern Ocean south of 30–40°S. Using independent information from ocean section estimates near 30–32°S (as in Wijffels 2001) gives an observed freshwater export from the Southern Ocean of 0.66 Sv. The ocean export of freshwater from the

Southern Ocean region in HadCM3 is also 0.66 Sv in the first decade, but some adjustment of the ocean transports to the model surface freshwater fluxes in this region (0.89 Sv for years 361–400) increases the ocean export to 0.97 Sv by years 361–400 (see Fig. 3). The model direct and implied exports of freshwater from the Southern Ocean for years 361–400 are at the higher end of, or greater than, the estimates from the noted observed ocean section estimates together with error bars from Wijffels (2001), also suggesting that the model surface freshwater flux into the Southern Ocean may be too high.

Wijffels (2001) notes that the scenario of inter-ocean exchange of freshwater suggested by using direct ocean observations differs from the scenario suggested by Wijffels et al. (1992) using surface flux observations (where there are large errors bars on the basin-scale convergences). Wijffels (2001) notes that in both scenarios the Indian Ocean is a significant evaporative basin. In the surface flux-based scenario, however, the Pacific Ocean is the major source of ocean freshwater for transport to highly evaporative Atlantic and Indian Oceans. The direct observations suggest, however, that the Atlantic is much less evaporative and that the net divergence of freshwater transport from the Pacific and the net convergence into the Arctic/Atlantic are small, with the Southern Ocean being the major source of freshwater for exchange with the evaporative Indian Ocean.

The basin-scale ocean freshwater transport convergences in the first decade of HadCM3, before major adjustment to the surface fluxes, are relatively strongly controlled by the temperature and salinity climatologies of Levitus and Boyer (1994), Levitus et al. (1994) and by the ocean model formulation. In the first decade of HadCM3, the small freshwater convergence into the Pacific suggests it plays a minor role in terms of net inter-ocean freshwater exchange, while the Southern Ocean is the major source of freshwater for the Indian Ocean and, to a lesser extent the Arctic/Atlantic, in much better agreement with the direct observation-based scenario proposed by Wijffels (2001), than with the surface flux-based observation scenario of Wijffels et al. (1992).

6.5 Summary of regional transports

A summary of the large-scale model freshwater budget discussed in this section is as follows. The model $P - E$ fluxes remain similar throughout the model run, consistent with the stable SSTs. In the lower latitudes, the largest differences between $P - E$ in the coupled model and $P - E$ from observations or from the atmosphere-only model, are related to errors in the coupled model SSTs. For both the atmosphere-only and coupled models, however, the observations suggest the models generally overestimate evaporation at lower latitudes and overestimate precipitation at higher latitudes, particularly in southern mid to high latitudes. Large section-integrated divergent components of model water vapour transport ($\tilde{Q}_D$), which link with the $P - E$ budget, are evident crossing from the Indian Ocean to the Pacific basin and from the Atlantic, Pacific and Indian oceans into the Southern Ocean. Water vapour is exported from the Atlantic (30°S to 66°N) by $\tilde{Q}_D$ along each of the boundary sections analysed, with much of this export compensated for by return runoff: the large divergent export westward over Amazonia does not enter the Pacific basin.

The total freshwater flux from river runoff into the ocean basins is generally close to observations. River runoff in HadCM3 from the western tropical–subtropical Atlantic coast, where river runoff from Amazonia in reality is particularly large, is underestimated, but an overestimate of runoff from the eastern side of the Atlantic largely balances this. There is too little sea-ice transported through Fram Strait, most probably because the ice is too thin. The model basin-scale ocean freshwater convergences are initially fairly consistent with the scenario proposed by Wijffels (2001) using ocean section measurements, but deviate from this later in the simulation (by years 361–400) as the model ocean increases the transport of freshwater from the Southern Ocean into the Atlantic to balance the model surface freshwater fluxes.

7 The Atlantic freshwater budget

The importance of the Atlantic freshwater budget for the thermohaline circulation, and the drifts in Atlantic salinity in HadCM3 led us to analyse the model Atlantic freshwater budget in more detail. The salinity and potential temperature drifts in the northern Atlantic region (as labelled in Fig. 10) are shown in Fig. 11. A fairly linear increase in the volume-weighted salinity is evident over the first 200 years, with the maximum area-averaged saline error found at 500–1000 m. The warm temperature drift errors follow a similar general pattern but with maximum errors at a deeper level. The drifts in potential density (not shown) initially follow the salinity drifts with higher densities developing in the upper 1000 m and spreading slowly to depth. The tropical–subtropical Atlantic region salinity, temperature and density drifts (not shown) are qualitatively similar to those in the northern Atlantic region, but take approximately 400 years to stabilise. The much slower drifts in Atlantic temperature and salinity that take place after year 400 (see Fig. 11) will not be discussed here as they are not the focus of this work.

Figure 12 shows the model implied and direct ocean freshwater transports in the Atlantic Ocean, relative to the freshwater transport through the Bering Strait, for years 1–10 and 361–400. The near balance of model direct and implied freshwater transports after 400 years, arising from an increase in oceanic freshwater convergence into the basin while the implied transports remain

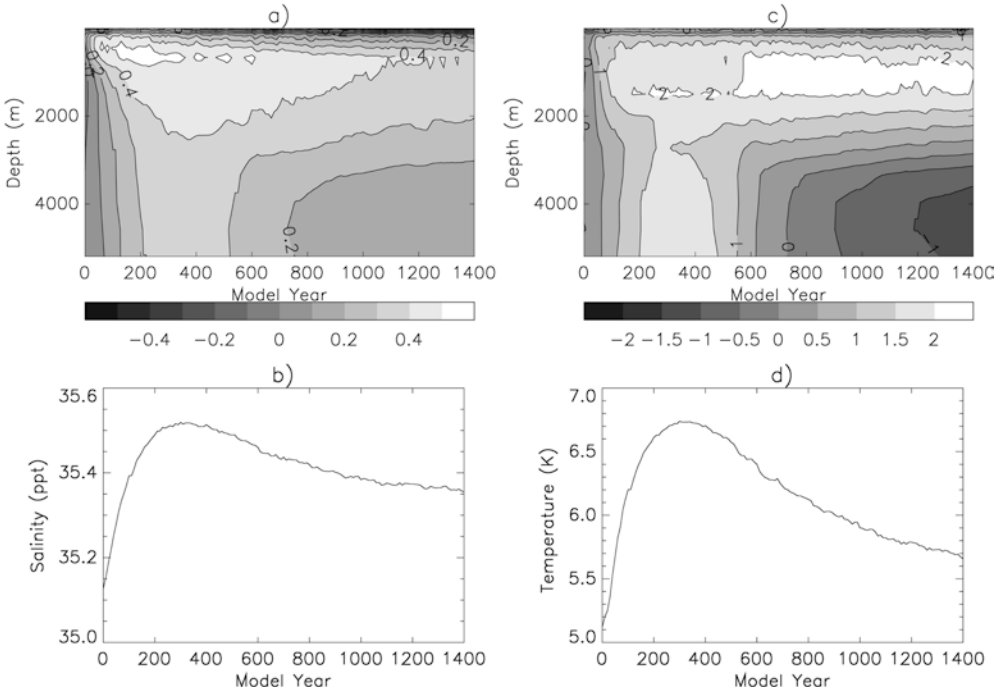

Fig. 11 For the HadCM3 northern Atlantic (region as labelled in Fig. 10) **a** area-averaged depth-time model salinity minus Levitus et al. (1994) climatology (contours every 0.1 psu), **b** volume-weighted model salinity (units psu) against time, **c** as **a** for model potential temperature minus Levitus and Boyer (1994) climatology (contours every 0.5 °K), **d** as **b** for model potential temperature (units °K)

stable, is again evident (the years 1–200 increase in salinity evident in Fig. 11b is the consequence of the initial imbalance in the northern Atlantic). Implied freshwater transport estimates calculated from the observed CMAP/O-SOC and Trenberth and Guillemot (1998) (TREN) $P - E$ climatologies with Baumgartner and Reichel (1975) runoff, and estimates derived from ocean section observations are also shown (see Sect. 4 for details). The implied transports given by TREN agree very well with the observed ocean section estimates, being within the error bars at all points except those of the Koltermann et al. (1999) estimates at 24°N. Wijffels (2001) noted that most observed ocean section estimates of freshwater transport for the ocean basins are in agreement with each other, given the estimated error bars. The 24°N estimates of Koltermann et al. (1999), however, are outliers from the range of observed Atlantic freshwater transport estimates shown by Wijffels (2001). The implied transports from the CMAP/O-SOC $P - E$ climatology are very similar to those from TREN over much of the northern hemisphere, but lead to smaller transports of freshwater into the Atlantic basin in the southern hemisphere, with estimates just outside of the direct estimate error bars near 30°S.

In the Northern Hemisphere Atlantic, north of about 20°N, Fig. 12 shows that the model implied freshwater transports are in good agreement with the observed implied and ocean section estimates (except the anomalously low estimates at 24°N of Koltermann et al. 1999). Comparing the model surface flux components with observations in this area (the region labelled as 'northern Atlantic' in Fig. 10) also shows fairly good agreement, with the model area-integrated precipitation and evaporation both being slightly higher (by about 0.1 Sv) than the CMAP/O and SOC estimates, and the runoff being within 0.005 Sv of an estimate derived from Baumgartner and Reichel (1975). Comparison of the model ocean freshwater convergence into the Northern Hemisphere of the Atlantic, with observed estimates from several of the ocean sections, and with the observed implied transports, suggests that in years 1–10 (and to a greater extent in the next few decades) the model ocean freshwater convergence may be too low (although it is close to the anomalously low 24°N estimates from Koltermann et al. 1999). Although the model starts from the Levitus and Boyer (1994) observed state, upper ocean salinity errors are evident in the first few years, and the model freshwater transports will be affected by these errors in the first decade.

In the Southern Hemisphere Fig. 12 shows that the implied model freshwater transports into the Atlantic are larger (outside of the error bars) in the first decade than the observed estimates from ocean sections, and although they decrease slightly during the simulation, they remain close to the upper limits of the ocean section error bars in years 361–400 (the change being mainly due to small increases, in runoff into the Arctic, and in $P - E$ into the tropical–subtropical Atlantic). This suggests that the model surface freshwater forcing in the Atlantic may be too negative when averaged across the basin. In the tropical–subtropical Atlantic region (as labelled in Fig. 10), the CMAP/O and SOC climatologies suggest that the model $P - E$ is too negative, due to the evaporation, by about 0.4 Sv (or 25% of the SOC evaporation). The Trenberth and Guillemot (1998) $P - E$ and the da Silva et al. (1994) adjusted (to be in global heat and freshwater balance) $P - E$ both suggest that the model $P - E$ is too negative in this region by about 0.2 Sv. The model tropical–subtropical Atlantic area-integrated runoff is a little lower (by about 0.04 Sv) than that from

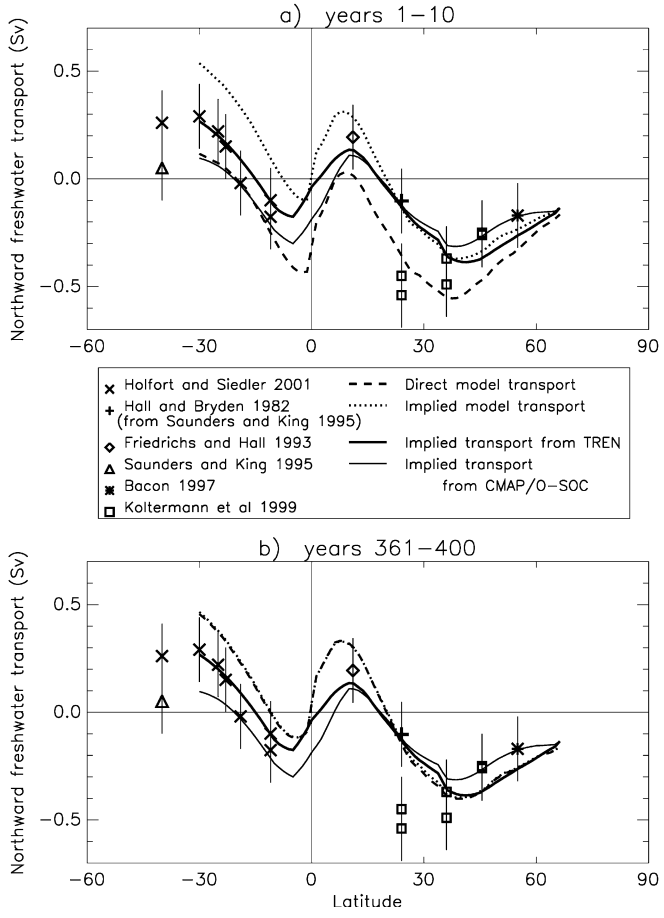

Fig. 12a, b HadCM3 Atlantic direct and implied northward freshwater transports (units Sv) relative to the freshwater transport through Bering Strait (F_b). *Symbols* show direct freshwater transport estimates derived from ocean sections with error bars of 0.15 Sv after Wijffels (2001). Implied freshwater transports from observed surface flux climatologies (see text for details) are also shown. Ocean section freshwater transports at 40°S are included as the section spans 30–45°S **a** years 1–10, **b** years 361–400

Baumgartner and Reichel (1975). In the first decade, before the adjustment of the model ocean freshwater transports, the model ocean freshwater convergence into the Atlantic basin (to 30°S) is slightly lower than estimates from ocean section measurements.

We have investigated possible reasons for the model Atlantic salinity drifts based on the differences suggested by our comparison between the Atlantic model freshwater budget and observations. There are a number of possible causes of a deficit of model ocean freshwater convergence into the Northern Hemisphere Atlantic. One possibility would be the lack of freshwater transported from Hudson/James bays and from the Baltic, but the integrated surface fluxes in these seas in the model only total 0.05 Sv (observational estimates suggest 0.03 Sv). Too little freshwater is transported from the model Atlantic to the Mediterranean (initially by about 0.03 Sv), so while this error no doubt forces much of the salinity drift in the Mediterranean, it should reduce the drift in the Atlantic. Another possibility is that the error is due to the lack of net freshwater flow through the Bering Strait in the model. A sensitivity study simulation parallel to the HadCM3 control, but where volume transport of water close to the observed magnitude was allowed through the Bering Strait, was run for twenty years. The northern Atlantic salinity drifts were reduced by about 25%, but the tropical–subtropical Atlantic salinity drifts increased and the salinity errors with depth in both regions remained similar to those in HadCM3.

A further possibility is that a deficit in Northern Hemisphere Atlantic northward freshwater transport is a consequence of a surface freshwater flux deficit in the tropical–subtropical Atlantic (suggested by the comparison with observations), which would then lead to overly saline water being transported northwards and therefore too small a northward freshwater flux. To investigate this possibility, two 20-year sensitivity study simulations were run. In the first experiment (experiment R_SST) the Atlantic SST was strongly relaxed to observed SST (Levitus and Boyer 1994) in just the tropical–subtropical region and in the second experiment (experiment R_SST/S) the Atlantic SST and SSS were both strongly relaxed to observed, again in just the tropical–subtropical region. The additional surface freshwater flux from the SSS relaxation corrects for errors in SSS due to errors in the surface fluxes and errors in the ocean model physics. Experiment R_SST shows that relaxing SST alone in the tropical–subtropical Atlantic makes little difference to the simulated salinity drifts over the 20 years. In experiment R_SST/S, however, the salinity drifts are significantly reduced throughout the Atlantic, with the northern Atlantic (where there is no relaxation) salinity drift reduced by about 75%. The additional surface freshwater flux (0.45 Sv) put in by the relaxation term (not shown) shows some small-scale features that are likely to be related to the positioning of the ocean currents, but on the larger scale freshwater is added to the ocean surface to reduce the subtropical evaporative maxima. This addition of surface freshwater reduces the implied northward freshwater transports in the Atlantic from those in HadCM3. The model direct ocean freshwater transports generally increase across the Atlantic, to be closer to the observed estimates in the Northern Hemisphere (with the exception of the 24°N Koltermann et al. 1999 estimates), but the freshwater convergence into the Atlantic basin as a whole remains similar (decreasing slightly near 30°S).

Experiment R_SST/S shows that correction of the model SSS in the tropical–subtropical region of the Atlantic can be achieved with an effective reduction in evaporation from the subtropical regions. This is consistent with the indications from observations that the model evaporation is too high. This additional freshwater reduces the difference between the model implied and direct ocean freshwater transports (so reducing the basin salinity drifts), and in general tends to bring the model implied and direct ocean transports

of freshwater closer to observations (with some exceptions which have been discussed). The ocean transport convergence of freshwater into the Atlantic basin as a whole, however, remains slightly lower than observed ocean section estimates (together with their error bars) near 30°S, suggesting that deficiencies in ocean transport may also play a role in the salinity drifts. In experiment R_SST/S, the Atlantic temperature drifts are also reduced from those in HadCM3 (whereas the drifts remain similar in experiment R_SST), suggesting that freshwater budget errors force some part of the temperature drifts.

8 The Atlantic freshwater budget and the thermohaline circulation

The Atlantic freshwater budget is likely to be crucial to the stability of the THC. Rahmstorf (1996) proposed that the ocean freshwater transport divergence associated with the equilibrium meridional overturning circulation in the Atlantic (to 30°S) is an indicator of the steady state stability regime of the THC; if the overturning circulation exports freshwater the THC is thermally driven and inhibited by surface freshwater input, whereas if the overturning circulation imports freshwater, the THC is driven by both thermal and haline components and is therefore in a more stable regime for a given temperature difference between the sinking region and 30°S. Weijer et al. (1999) have also looked at the overturning component of the freshwater transport at 30°S using results from an inverse model and WOCE data. Their analysis finds, as suggested by Rahmstorf (1996), that the present-day overturning circulation exports freshwater from the Atlantic.

Figure 13 shows the implied and direct ocean freshwater convergences in the model Atlantic for years 1–10 and years 361–400 (as in Fig. 12), with the overturning (zonal-mean) and gyre (deviation from the zonal-mean) components of the ocean freshwater transport also shown (the total ocean transport also includes a contribution from diffusion). Figure 13 shows that the increase in oceanic freshwater convergence between 30°S and the Bering Strait (equivalent to an increased divergence of salinity), which brings the model freshwater transports into near balance with the surface fluxes, is largely accomplished by the overturning circulation. Figure 14 indicates the changes that have taken place in the zonal-mean salinity to achieve this balance. Increases in zonally-averaged salinity over the 400 year period (Fig. 14a, b), which lead to large saline errors relative to Levitus et al. (1994, Fig. 14c) are evident at most depths, but the ocean is too fresh in the zonal-mean in the upper 1000 m south of 20°S. The changes evident in Figs. 13a, b and 14a, b between years 1–10 and years 361–400 suggest that the Atlantic saline drift continues until overly saline near-surface water (consistent with an overestimate of evaporation) advected northwards from

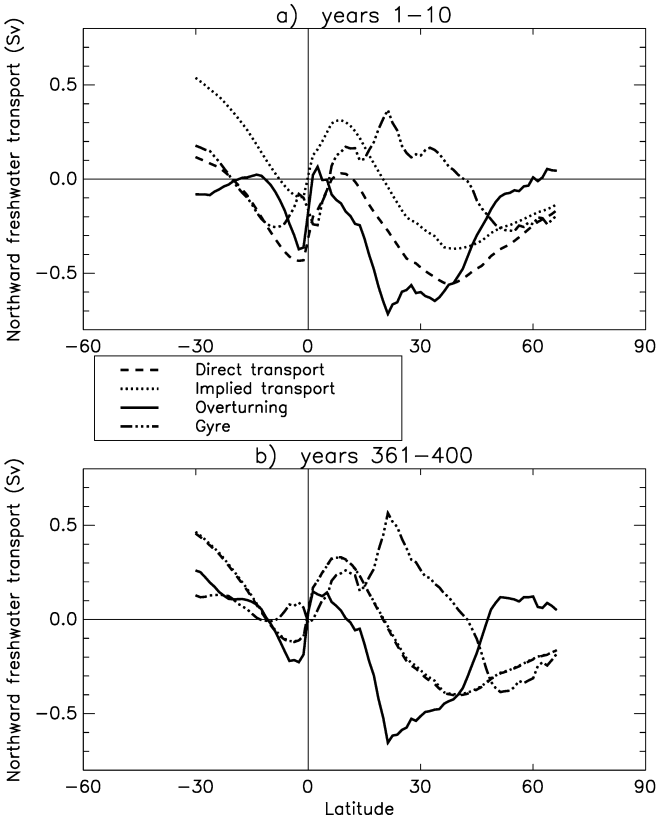

Fig. 13a, b HadCM3 Atlantic overturning (zonal-mean) and gyre components of northward freshwater transport (units Sv) shown with the model Atlantic total ocean (including diffusive component) and implied freshwater transports (as in Fig. 12). All transports are relative to Bering Strait **a** years 1–10, **b** years 361–400

the subtropical Atlantic has sunk to depth and changed the properties of the volume of water which forms the southwards travelling North Atlantic Deep Water (NADW), exiting the Atlantic at 30°S, therefore increasing the salinity divergence and the freshwater convergence. Overly fresh upper and intermediate water from the Southern Ocean (consistent with an overestimate of precipitation at high latitudes) also plays a role in increasing freshwater convergence into the basin.

The total ocean freshwater transport convergence into the Atlantic basin in the initial decade is slightly less (within 0.1 Sv) than that from the global ocean model of Rahmstorf (1996) and approximately 0.2 Sv less than that from the inverse model of Schiller (1995) that he refers to. The overturning component of the HadCM3 freshwater transport in the initial decade gives a divergence of nearly 0.1 Sv out of the Atlantic, similar in magnitude to that from the Schiller (1995) inverse model, but the HadCM3 overturning component of freshwater transport changes to a convergence of 0.25 Sv by years 361–400. The change, over the long model adjustment time period, from net export of freshwater by the overturning circulation from the Atlantic to net import, could suggest, by comparison

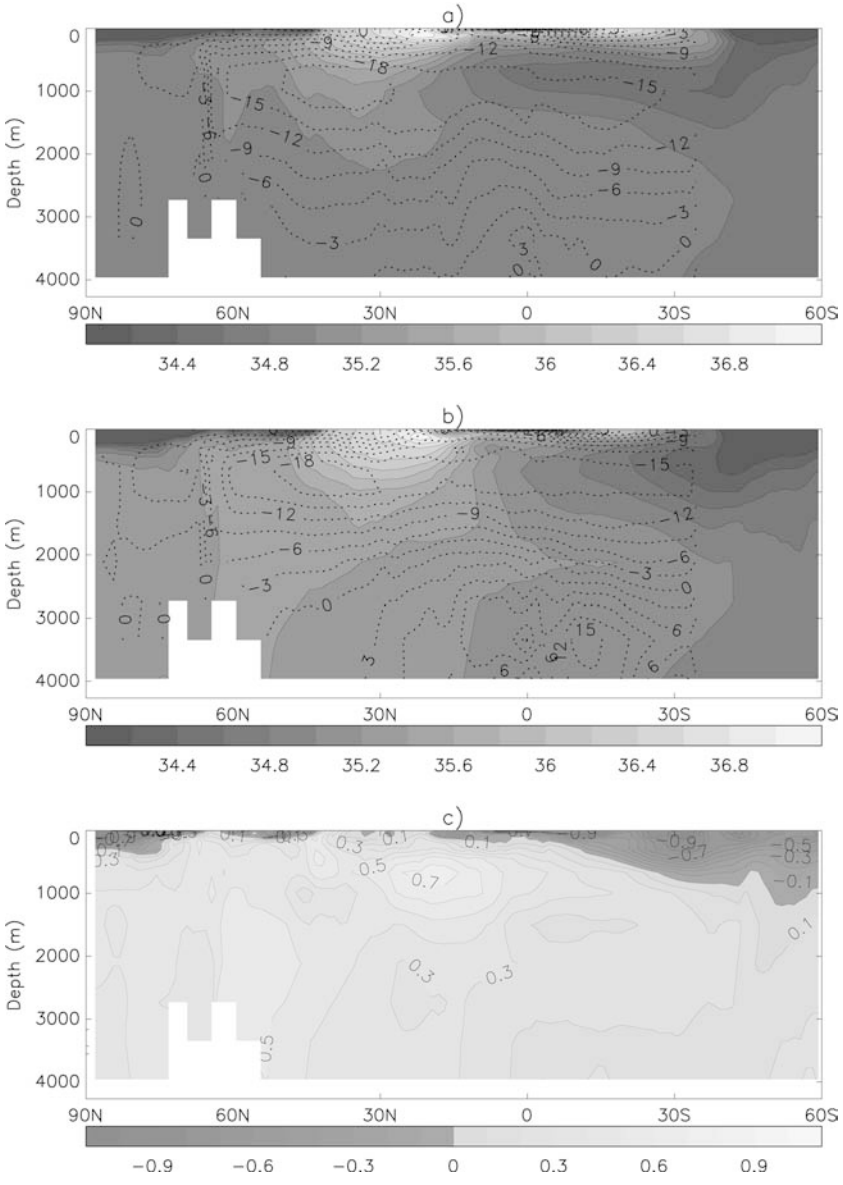

Fig. 14 Zonal-mean salinity across Arctic, northern Atlantic, tropical–subtropical Atlantic and Atlantic Southern Ocean regions (as labelled in Fig. 10) **a** HadCM3 salinity (in greyscale, contours every 0.2 psu) overlaid with Atlantic overturning stream function (dotted contours every 3 Sv) for years 1–10 **b** as **a** for years 361–400, **c** HadCM3 (years 361–400) minus Levitus et al. (1994) salinity error (contours every 0.1 psu)

with the conceptual model of Rahmstorf (1996), that the HadCM3 control run is tending to an equilibrium state where the THC is driven by both thermal and freshwater forcing and may therefore be in a more stable state than the 'present-day' conditions identified in Rahmstorf (1996) in which the THC is purely thermally driven. However Saenko et al. (2002) caution that the overturning concept of freshwater transport cannot necessarily be attributed to the thermohaline circulation. Moreover, in the HadCM3 control run, the temperature drifts are also likely to influence the model THC stability and strength. It should also be noted that Rahmstorf (1996) emphasises that it is the equilibrium THC that is related to the freshwater surface flux input to the Atlantic basin (to 30°S), while changes in the distribution of surface freshwater fluxes within the Atlantic basin are important for the transient response. The extent to which this possible overestimate of equilibrium THC stability due to the freshwater budget errors in HadCM3 might be important for more transient THC behaviour, such as might occur under greenhouse gas warming conditions, is unclear.

9 Summary and conclusions

Changes to the hydrological cycle, such as those which might occur in a greenhouse warming scenario, are potentially serious, both because of consequences for water availability, and because of the many ways in which the hydrological cycle influences climate. The evaluation of the simulation of the hydrological cycle in climate models is therefore important. Observations of the hydrological cycle are limited, particularly over the oceans, and so there is considerable uncertainty in the magnitude of the components of ocean basin freshwater budgets. Increased availability of freshwater transport estimates from ocean sections, however, has improved

the ability to evaluate the hydrological cycle in general circulation models. The self-consistent hydrological cycle represented by ocean–atmosphere coupled climate models run without flux adjustments (which introduce artificial moisture transports) allow for the limited observations of freshwater budget components to be interpreted in the context of a global model cycle. We have analysed and evaluated large-scale aspects of the freshwater budget over the global ocean in a simulation of over 1000 years using the HadCM3 coupled climate model.

Many aspects of the freshwater cycle in HadCM3 have been shown to be well represented. Pope et al. (2000) noted that the simulation of precipitation in the atmosphere-only model is generally good and has similar errors to those from the mean of the ensemble of models participating in AMIP I. Many aspects of the large-scale precipitation and evaporation in this atmosphere-only model run are similar to those in the coupled model. The decadal mean surface freshwater fluxes in HadCM3 remain similar during the course of the simulation, consistent with the fairly stable sea surface temperature and sea-ice extents. The observational data we have used suggest that the hydrological cycle in the HadCM3 control run may be somewhat too strong, with an overestimate of precipitation, particularly at the mid to higher southern latitudes, and an overestimate of evaporation at tropical to subtropical latitudes. The HadCM3 basin-scale meridional ocean transports of freshwater adjust to the model surface fluxes over a period of about 400 years. The major change in the global mean meridional freshwater transports is an increased relative northward transport of freshwater in the Southern Hemisphere and in the lower latitudes of the Northern Hemisphere.

We have looked at the HadCM3 Atlantic freshwater budget in more detail and, consistent with the global picture, comparison with observations and sensitivity studies have suggested that the model overestimates evaporation at the lower latitudes, and that this is likely to be the dominant cause of the drift to more saline conditions in the model Atlantic Ocean, although other freshwater budget components may also play a role. The river runoff in the coupled model from the west coast of the tropical–subtropical Atlantic is too low, but there is partial compensation for this in the low latitudes of the Atlantic Ocean, by an excess of runoff from the West African coast. The transport of sea-ice across Fram Strait, is also somewhat underestimated. The ocean northward transports of freshwater over much of the Northern Hemisphere Atlantic, relative to that through Bering Strait, are initially too low compared with most observations, but we suggest much of this is a response to a surface flux error, with water that is too saline then being transported northwards. The ocean transport freshwater convergence into the Atlantic basin to 30°S, however, is also a little lower than direct estimates and ocean model errors may contribute to the Atlantic salinity drifts.

In the initial decade of the HadCM3 simulation, the basin-scale ocean freshwater transport convergences are fairly consistent with the scenario suggested by Wijffels (2001) from direct ocean section measurements, with the major ocean basin export of freshwater being from the Southern Ocean to the Indian Ocean. The likely overestimates of evaporation in the model tropical–subtropical Atlantic and of precipitation at higher southern latitudes lead to an increase in ocean freshwater transport from the Southern Ocean, predominantly into the Atlantic, as the simulation progresses. This change in ocean freshwater transport into the Atlantic basin is largely accomplished by the overturning circulation component which changes from a net export to a net import of freshwater to the Atlantic basin. The implications of the model Atlantic ocean freshwater transports, if related to the conceptual model and present-day stability of the THC suggested by Rahmstorf (1996), are that as the model ocean freshwater transports come into balance with the surface freshwater fluxes, the equilibrium THC may be too stable relative to present day conditions. This possibility and any implications for more transient changes to the THC, such as may occur under greenhouse gas warming and for which processes not included in the model of Rahmstorf (1996) may be important, require further investigation.

The heat transports into the Atlantic basin by years 361–400 of the HadCM3 control run were shown to be near observed by Gordon et al. 2000, (see their Figs. 18, 19b), although there is significant variation in the observed estimates. They found that shortwave radiative heat gains by the ocean were larger in the model than in the da Silva et al. (1994) adjusted climatology, which led to some cancellation with the overestimated latent heat losses in the model relative to da Silva et al. (1994). This would allow equilibrium heat transports into the Atlantic to be near observed while requiring the freshwater transports to be too high in order to balance a model excess of evaporation, as found here.

Collins (2001) looked at the issue of partition of solar absorption between the atmosphere and surface in the tropical climate system in the context of the suggestion that models may underestimate solar absorption by the atmosphere. A tendency for models to overestimate surface shortwave fluxes and the need, if these were to be reduced, to reduce the latent heat flux loss from the oceans in order to maintain surface energy balance was noted. Slingo (2002) noted that there is considerable uncertainty in the estimates of solar absorption by the atmosphere, but comparison with estimates derived from satellite measurements and direct surface radiation budget estimates suggest that models might still underestimate the absorption by up to about 10 $W\,m^{-2}$ globally, possibly due to a deficit of absorption by gases, aerosols or clouds. If this is the case, this suggests that an overly strong hydrological cycle may be a generic problem for model simulations. The atmosphere-only part of HadCM3, driven with prescribed SSTs, is known (Pope et al. 2000) to have too strong Hadley and Walker

circulations which are consistent with an overactive hydrological cycle. Gaffen et al. (1997) looked at the moisture budgets of the atmosphere-only models participating in AMIP I and concluded that most models overestimated the poleward flux of moisture relative to observations. The conclusions we come to here as to the source of the model Atlantic salinity drift and errors in the hydrological cycle are based on a number of factors. We have used a combination of comparison against surface flux measurements, direct ocean section measurement estimates, salinity climatology and model sensitivity studies. Improved freshwater flux datasets, such as may be obtained from more numerous ocean section measurements and the further use of inverse models, will be needed to enable our conclusions to be stated with increased confidence.

Acknowledgements We thank Susan Wijffels for providing us with an early draft of Wijffels (2001). We acknowledge Howard Cattle for comments on the original manuscript and Richard Wood, Peter Cox, Chris Gordon, Tony Slingo, William Ingram, John Edwards and Simon Josey for useful discussions. We would like to thank the reviewers for their helpful comments. This work was funded by the Department of the Environment, Food and Rural Affairs Climate Prediction Programme (contract PECD 7/12/37) and by the Government Meteorological Research Programme.

Appendix 1

1.1 Implications of the rigid-lid formulation for salinity

Because of its unrealistic requirement of zero volume divergence, the ocean model rigid-lid approximation obviously introduces errors in the velocities. However, the simulation of large-scale ocean volume transports appears to be acceptable (e.g. Wood et al. 1999; Vellinga et al. 2002). This is possible because typical large-scale volume transports are of order (1–100) Sv, while freshwater divergences from large regions (the cause of volume divergence in the real world) are typically a few tenths of a Sv (Wijffels et al. 1992; Wijffels 2001). Hence the distortion of transports implied by the rigid lid is fractionally small.

Even if F_s has zero global average, Eq. 3 allows a drift in global volume-integrated salinity, because the geographical covariance of S_* and ρ_* with F_s can lead to a non-zero global average for $-(S_*/\rho_*)F_s$. Therefore a constant reference salinity $S_* = 35$ psu and density $\rho_* = 1026$ kg m^{-3} are used instead. The use of the reference salinity means that freshwater fluxes will have a larger effect on the surface salinity in the model than in reality at locations where the reference salinity S_* is larger than the local S, and a smaller effect where $S_* < S$. Areas where the net freshwater flux is into the ocean ($F_s > 0$) tend to be colocated with areas where its effect on salinity in the model is enhanced, because the sea surface salinity is fresher than average ($S_0 > S$). Areas where $F_s < 0$ tend to coincide with areas where the effect on salinity is suppressed, because $S_* < S$. Hence the use of a reference salinity will generally tend to freshen most areas of the sea surface. However, calculations suggest that the errors in model F_s relative to observations generally have a much larger influence.

References

Aagaard K, Carmack EC (1989) The role of sea ice and other fresh water in the Arctic circulation. J Geophys Res 94: 14,485–14,498

Bacon S (1997) Circulation and fluxes in the North Atlantic between Greenland and Ireland. J Phys Oceanogr 27: 1420–1435

Baumgartner A, Reichel E (1975) The world water balance. Elsevier, Amsterdam

Bryden H, Candela J, Kinder T (1994) Exchange through the Strait of Gibraltar. Prog Oceanogr 33: 201–248

Cattle H, Cresswell D (2000) The Arctic Ocean freshwater budget of a climate general circulation model. In: Lewis EL, et al. (ed) The freshwater budget of the Arctic Ocean 127–139 Kluwer Academic, The Netherlands

Chahine M (1992) The hydrological cycle and its influence on climate. Nature 359: 373–380

Chen TC, Pfaendtner J, Weng SP (1994) Aspects of the hydrological cycle of the ocean–atmosphere system. J Phys Oceanogr 24: 1827–1833

Coachman L, Aagaard K (1988) Transports through Bering Strait: annual and interannual variability. J Geophys Res 93: 15,535–15,539

Collins W (2001) Effects of enhanced shortwave absorption on coupled simulations of the tropical climate system. J Clim 14: 1147–1165

Cox PM, Betts RA, Jones CD, Spall SA, Totterdell IJ (2000) Acceleration of global warming due to carbon–cycle feedbacks in a coupled climate model. Nature 408: 184–187

Cox MD (1984) A primitive equation, three dimensional model of the ocean. Ocean Group Technical Report 1, GFDL Princeton, USA

da Silva A, Young C, Levitus S (1994) Atlas of surface marine data, vol 1: algorithms and procedures. NOAA atlas series

Delire C, Calvet J, Noilhan J, Wright I, Manzi A, Nobre C (1997) Physical properties of Amazonian soils: a modeling study using the Anglo-Brazilian Climate Observation Study data. J Geophys Res 102(D25): 30,119–30,133

Eilola K, Stigebrandt A (1998) Spreading of juvenile freshwater in the Baltic proper. J Geophys Res 103(C12): 27,795–27,807

Fichefet T, Morales-Maqueda MA (1997) Sensitivity of a global sea ice model to the treatment of ice thermodynamics and leads. J Geophys Res 102: 12,609–12,646

Friedrichs M, Hall M (1993) Deep circulation in the tropical North Atlantic. J Mar Res 51: 697–736

Gaffen D, Rosen R, Salstein D, Boyle J (1997) Evaluation of tropospheric water vapor simulations from the Atmospheric Model Intercomparison Project. J Clim 10: 1648–1661

Gedney N, Cox P, Douville H, Polcher J, Valdes P (2000) Characterizing GCM land-surface schemes to understand their responses to climate change. J Clim 13: 3066–3079

Gent PR, McWilliams JC (1990) Isopycnal mixing in ocean circulation models. J Phys Oceanogr 20: 150–155

Gordon C, Cooper C, Senior CA, Banks H, Gregory JM, Johns TC, Mitchell JFB, Wood RA (2000) The simulation of SST, sea ice extents and ocean heat transports in a version of the Hadley Centre coupled model without flux adjustments. Clim Dyn 16: 147–168

Gregory JM, Stott PA, Cresswell DJ, Rayner NA, Gordon C, Sexton DMH (2002) Recent and future changes in Arctic sea ice simulated by the HadCM3 AOGCM. Geophys Res Lett 29(24): 2175

Hall MM, Bryden HL (1982) Direct estimates and mechanisms of ocean heat transport. Deep-Sea Res 29: 339–359

Harder M, Lemke P, Hilmer M (1998) Simulation of sea ice transport through Fram Strait: natural variability and sensitivity to forcing. J Geophys Res 103: 5595–5606

Hibler WD (1979) A dynamic thermodynamic sea ice model. J Phys Oceanogr 9: 815–846

Holfort J, Siedler G (2001) The meridional oceanic transports of heat and nutrients in the South Atlantic. J Phys Oceanogr 31: 5–29

Josey S, Kent E, Taylor P (1999) New insights into the ocean heat budget closure problem from analysis of the SOC air-sea flux climatology. J Clim 12: 2856–2880

Koltermann K, Sokov A, Tereschenkov V, Dobroliubov S, Lorbacher K, Sy A (1999) Decadal changes in the thermohaline circulation of the North Atlantic. Deep-Sea Res 46: 109–138

Latif M, Roeckner E, Mikolajewicz U, Voss R (2000) Tropical stabilization of the thermohaline circulation in a greenhouse warming simulation. J Clim 13: 1809–1813

Levitus S, Boyer TP (1994) World ocean atlas 1994, volume 4: Temperature. NOAA/NESDIS E/OC21. US Department of Commerce, Washington, DC, USA, pp 117

Levitus S, Burgett R, Boyer TP (1994) World ocean atlas 1994, volume 3: Salinity. NOAA/NESDIS E/OC21. US Department of Commerce, Washington, DC, USA, pp 99

Manabe S, Stouffer RJ (1994) Multiple century response of a coupled ocean–atmosphere model to an increase of atmospheric carbon dioxide. J Clim 7: 5–23

Miller JR, Russell GL (2000) Projected impact of climate change on the freshwater and salt budgets of the Arctic Ocean by a global climate model. Geophys Res Lett 27: 1183–1186

NSIDC (1989) DMSP SSM/I brightness temperatures and sea ice concentration grids for the polar regions. NSIDC Distributed Active Archive Centre, University of Colorado, Boulder, USA

Pope VD, Gallani ML, Rowntree PR, Stratton RA (2000) The impact of new physical parametrizations in the Hadley Centre climate model – HadAM3. Clim Dyn 16: 123–146

Prinsenberg S (1980) Man-made changes in the freshwater input rates of Hudson and James Bays. Can J Fish Aqu 37: 1101–1110

Rahmstorf S (1995) Bifurcations of the Atlantic thermohaline circulation in response to changes in the hydrological cycle. Nature 378: 145–149

Rahmstorf S (1996) On the freshwater forcing and transport of the Atlantic thermohaline circulation. Clim Dyn 12: 799–811

Rahmstorf S (2000) The thermohaline circulation: a system with dangerous thresholds? Clim Change 46: 247–256

Saenko OA, Gregory JM, Weaver AJ, Eby M (2002) Distinguishing the influences of heat, freshwater and momentum fluxes on ocean circulation and climate. J Clim 15: 3686–3697

Saunders P, King B (1995) Oceanic fluxes on the WOCE A11 section. J Phys Oceanogr 25: 1942–1958

Schiller A (1995) The mean circulation of the Atlantic Ocean north of 30S determined with the adjoint method applied to an ocean general circulation model. J Mar Res 53: 453–497

Semtner AJ (1976) A model for the thermodynamic growth of sea ice in numerical investigations of climate. J Phys Oceanogr 6: 379–389

Slingo A (2002) Meteorology at the Millennium, cha. Absorption of solar radiation in the atmosphere: reconciling models with measurements, Academic Press, New York, pp 165–173

Sloyan B, Rintoul S (2001) The Southern Ocean limb of the global deep overturning circulation. J Phys Oceanogr 31: 143–173

Steele M, Zhang J, Rothrock D, Stern H (1997) The force balance of sea ice in a numerical model of the Arctic Ocean. J Geophys Res 102: 21,061–21,079

Thorpe RB, Gregory JM, Johns TC, Wood RA, Mitchell JFB (2001) Mechanisms determining the Atlantic thermohaline circulation response to greenhouse gas forcing in a non-flux-adjusted coupled climate model. J Clim 14: 3102–3116

Trenberth K, Guillemot C (1998) Evaluation of the atmospheric moisture and hydrological cycle in the NCEP/NCAR reanalyses. Clim Dyn 14: 213–231

UNESCO (1971) Discharge of selected rivers of the world. Studies and reports in hydrology 5, UNESCO

Vellinga M, Wood RA (2002) Global climatic impacts of a collapse of the Atlantic thermohaline circulation. Clim Change 54(3): 251–267

Vellinga M, Wood RA, Gregory JM (2002) Processes governing the recovery of a perturbed thermohaline circulation in HadCM3. J Clim 15(7): 764–780

Vinje T, Nordlund N, Kvambekk Å (1998) Monitoring ice thickness in Fram Strait. J Geophys Res 103: 10,437–10,449

Weijer W, de Ruijter W, Dijkstra H, van Leeuwen P (1999) Impact of interbasin exchange on the Atlantic overturning circulation. J Phys Oceanogr 29: 2266–3184

Wijffels SE, Schmitt RW, Bryden HL, Stigebrandt A (1992) Transport of freshwater by the oceans. J Phys Oceanogr 22: 155–162

Wijffels SE (2001) Ocean transport of freshwater. In: Ocean circulation and climate. Academic Press, New York, pp 475–488

Wood RA, Keen AB, Mitchell JFB, Gregory JM (1999) Changing spatial structure of the thermohaline circulation in response to atmospheric CO_2 forcing in a climate model. Nature 399: 572–575

Xie P, Arkin PA (1997) Global precipitation: a 17-year monthly analysis based on gauge observations, satellite estimates and numerical model outputs. Bull Am Meteorol Soc 78(11): 2539–2558

Zaucker F, Stocker T, Broecker W (1994) Atmospheric freshwater fluxes and their effect on the global thermohaline circulation. J Geophys Res 99(c6): 12,443–12,457